

Multiscale Topology in Interatomic Network: From Transcriptome to Antiaddiction Drug Repurposing

Hongyan Du^{1,2} and Guo-Wei Wei^{2,3,4*} and Tingjun Hou^{1†}

¹ College of Pharmaceutical Sciences,
Zhejiang University, Hangzhou 310058, Zhejiang, China.

² Department of Mathematics,
Michigan State University, MI 48824, USA.

³ Department of Electrical and Computer Engineering,
Michigan State University, MI 48824, USA.

⁴ Department of Biochemistry and Molecular Biology,
Michigan State University, MI 48824, USA.

December 5, 2023

Abstract

The escalating drug addiction crisis in the United States underscores the urgent need for innovative therapeutic strategies. This study embarked on an innovative and rigorous strategy to unearth potential drug repurposing candidates for opioid and cocaine addiction treatment, bridging the gap between transcriptomic data analysis and drug discovery. We initiated our approach by conducting differential gene expression analysis on addiction-related transcriptomic data to identify key genes. We propose a novel topological differentiation to identify key genes from a protein-protein interaction (PPI) network derived from DEGs. This method utilizes persistent Laplacians to accurately single out pivotal nodes within the network, conducting this analysis in a multiscale manner to ensure high reliability. Through rigorous literature validation, pathway analysis, and data-availability scrutiny, we identified three pivotal molecular targets, mTOR, mGluR5, and NMDAR, for drug repurposing from DrugBank. We crafted machine learning models employing two natural language processing (NLP)-based embeddings and a traditional 2D fingerprint, which demonstrated robust predictive ability in gauging binding affinities of DrugBank compounds to selected targets. Furthermore, we elucidated the interactions of promising drugs with the targets and evaluated their drug-likeness. This study delineates a multi-faceted and comprehensive analytical framework, amalgamating bioinformatics, topological data analysis and machine learning, for drug repurposing in addiction treatment, setting the stage for subsequent experimental validation. The versatility of the methods we developed allows for applications across a range of diseases and transcriptomic datasets.

Keywords: Substance addiction, Differentially expressed gene, Persistent spectral theory, Drug repurposing

*Corresponding author. Email: weig@msu.edu

†Corresponding author. Email: tingjunhou@zju.edu.cn

Contents

1	Introduction	1
2	Results and Discussion	4
2.1	Opioid Addiction Analysis	4
2.1.1	Differential expression analysis	4
2.1.2	Multiscale topological differentiation of PPI networks	6
2.1.3	Literature validation	8
2.1.4	Pathway enrichment	8
2.2	Cocaine Addiction Analysis	9
2.2.1	Differential expression analysis and key genes identification	9
2.2.2	Literature validation	10
2.2.3	Pathway enrichment	11
2.3	Integrated Analysis of Opioid and Cocaine Addiction DEGs	11
2.3.1	Literature validation	12
2.4	Repurposing of DrugBank for addiction-related targets	13
2.4.1	Binding affinity predictors for addiction-related targets	13
2.4.2	Potential inhibitors of addiction-related targets in DrugBank	13
2.4.2.1	Approved drugs with predicted efficacy on mTOR	13
2.4.2.2	Investigational drugs with predicted efficacy on mTOR	15
2.4.2.3	Approved drugs with predicted efficacy on mGluR5	16
2.4.2.4	Investigational drugs with predicted efficacy on mGluR5	18
2.4.2.5	Approved drugs with predicted efficacy on NMDAR	19
2.4.2.6	Investigational drugs with predicted efficacy on NMDAR	20
2.4.3	ADMET analysis	21
3	Methods	22
3.1	DEG analysis and PPI network	22
3.2	Multiscale topological differentiation of network	22
3.2.1	Persistent spectral theory	23
3.2.2	Persistent homology	24
3.2.3	Key gene identification via network topological differentiation	24
3.3	Machine learning-based drug repurposing	25
3.3.1	Data preparation	25
3.3.2	Molecular fingerprints	25
3.3.2.1	Bidirectional transformer	25
3.3.2.2	Sequence-to-sequence auto-encoder	25
3.3.2.3	Extended-connectivity fingerprints	26
3.3.3	Machine learning models	26
4	Conclusion	26
5	Data Availability	27
6	Acknowledgements	27
7	Conflicts of Interests	27
	Appendices	28

Appendix A Literature validation	28
A.1 Opioid addiction-related key genes	28
A.2 Cocaine addiction-related key genes	29
A.3 Integrated Analysis of Opioid and Cocaine Addiction	29
Appendix B Topological objects	30
B.1 Simplicial complex and chain complex	30
B.2 q -combinatorial Laplacian	32
Appendix C Datasets for machine learning	33
Appendix D Evaluation metrics	34
Appendix E Gene significance ranking	34

1 Introduction

The ongoing drug addiction crisis presents a severe global public health challenge, particularly in the United States (US). The startling statistics from the US National Center for Drug Abuse Statistics shows that as of 2020, 37.309 million individuals aged 12 and older were identified as current illegal drug users, with a cumulative nearly one million drug overdose deaths recorded since 2000. The economic burden is significant, with \$35 billion allocated for drug control in 2020. Moreover, the mortality associated with drug addiction is harrowing, with nearly 92,000 drug overdose deaths recorded in 2020 alone. Among the diverse substances abused, opioids and cocaine are two predominant agents exacerbating the addiction epidemic.

The term “opioid” encompasses both natural and synthetic substances that bind to specific opioid receptors within the human body. Misuse of opioids can lead to opioid use disorder (OUD), characterized by cravings, continued use despite physical and/or psychological decline, increased tolerance, and withdrawal symptoms upon cessation [1]. Opioids interact primarily with three receptors in the central nervous system (CNS) and peripheral organs: the mu opioid receptor (MOR), kappa opioid receptor (KOR), and delta-opioid receptor (DOR), regulating various physiological functions including analgesia, respiration, and hormonal regulation [2]. Synthetic and exogenous opioids (e.g., morphine, heroin, oxycotin) mimic endorphins in their action on opioid receptors, with repeated and escalating use inducing gradual brain adaptations.

The United States Food and Drug Administration (FDA) has approved three medications for opioid dependency management: methadone, buprenorphine, and naltrexone. Methadone, a full MOR agonist, alleviates withdrawal and craving symptoms, proving beneficial in methadone maintenance treatment (MMT) to mitigate withdrawal severity and deter additional opioid intake for euphoria. While MMT aids in reducing cravings, facilitating treatment retention, methadone carries a risk of respiratory depression if misadministered [3]. Buprenorphine is a partial MOR agonist and serves as an alternative to methadone. It has a ceiling effect on MOR stimulation, offering less euphoria and a lower risk of respiratory depression [4]. Naltrexone is an MOR antagonist that effectively reduces drug cravings and the risk of overdose without inducing sedation, analgesia, or euphoria [5]. However, its usage is less common due to lower patient acceptance and adherence. While current medications effectively manage OUD to an extent, relapse and remission are prevalent due to the neurobiological shifts and opioid receptor tolerance from repeated abuse. The identification of new therapeutic targets and corresponding drug development is anticipated to alleviate the challenges encountered in OUD treatment.

Cocaine is a tropane alkaloid stimulant known for its high addictive potential. Its misuse leads to serious health complications, including an increased risk of human immunodeficiency virus (HIV), hepatitis B, and heart disease. Additionally, it is associated with a rise in crime and violence rates [6]. Cocaine exerts its effects by binding to three monoamine transporters: dopamine transporter (DAT), serotonin transporter (SERT), and norepinephrine transporter (NET) [7–9]. This binding action inhibits neurotransmitter reuptake, leading to elevated synaptic neurotransmitter levels and enhanced euphoric experiences. Specifically, cocaine’s blockade of DAT increases dopamine levels in the synaptic cleft, which in turn stimulates dopamine receptors in the postsynaptic neuron, generating euphoria and arousal [10]. The D3 dopamine receptor (D3R) in the mesolimbic reward system plays a crucial role in cocaine’s rewarding and addictive effects [11]. In vivo studies reveal that acute cocaine intoxication boosts serotonin release, whereas withdrawal leads to decreased serotonin levels in the nucleus accumbens [12]. NET, embedded in the plasma membrane of noradrenergic neurons, serves as a primary conduit for the inactivation of noradrenergic signaling by reabsorbing synaptically released norepinephrine (NE). Preclinical research highlights the role of the noradrenergic system in stress-induced reinstatement of cocaine seeking behavior [13]. Some clinical studies suggest that adrenergic blockers might offer a potential treatment pathway, especially for individuals with severe cocaine withdrawal symptoms [14]. Despite ongoing research efforts, the FDA has not

approved any effective medication for treating cocaine dependence.

Differentially Expressed Gene (DEG) analysis is a crucial tool in molecular biology and genetics, showing promise in identifying new targets for drug addiction treatment, and aiding in discovering novel therapeutic agents. By exploring the transcriptomic dynamics underlying various biological conditions including drug addiction, DEG analysis allows researchers to examine transcriptomic datasets and identify genes with significantly altered expression levels under different conditions or between varying sample groups. Comparing gene expression profiles between drug-exposed and control groups unveils potential molecular mechanisms driving addictive behaviors or responses to substances of abuse. Zhang et al. have delineated biomarkers for opioid addiction through integrated bioinformatics analysis of gene expression data from heroin addicts [15]. Similarly, Wang et al. employed this approach to explore cocaine addiction and suggest potential therapeutic drugs targeting key genes, as identified through database analysis [16]. Despite their valuable insights, these studies primarily rely on central algorithms for key gene identification from DEGs' PPI networks. These algorithms focus predominantly on connection relationships within the network, often neglecting the quantitative assessment of interaction confidence or strength, thereby potentially missing critical information. Furthermore, these methods are traditionally limited in handling only the low-dimensional connections of data, which may result in an incomplete understanding of the complex, high-dimensional nature of PPI networks. Moreover, despite identifying key genes, these studies did not employ quantitative methodologies to drive drug discovery efforts targeting the identified genes.

Topological Data Analysis (TDA) introduces a groundbreaking perspective in analyzing these intricate biological networks. Within TDA, persistent homology stands out as a powerful tool, applying algebraic topology to uncover topological features such as holes and voids [17]. This technique facilitates a multi-scale analysis through its filtration process, generating a series of topological invariants that uniquely characterize data. However, persistent homology does not account for the homotopic shape evolution of data, a limitation addressed by persistent spectral graph (PST), also called persistent Laplacians [18]. PST encompasses both harmonic and non-harmonic spectra, where the former recovers all topological invariants from persistent homology, and the latter reveals the homotopic shape evolution. It represents PPI networks in a topological space and adeptly captures both the overarching structure and subtle local interactions within the PPI network. PST has been successfully employed in various applications, including machine learning-assisted protein engineering predictions [19], forecasting dominant SARS-CoV-2 variants [20], predicting protein-ligand binding affinity [21], drug addiction analysis [22], and in dimensionality reduction for gene expression data [23].

Investigating existing drugs for new therapeutic prospects beyond their initially intended applications, a process known as drug repurposing, has yielded successful outcomes in several scenarios, providing a pathway to diminish development costs and expedite timelines [24]. In the wake of the proliferation of biological data, machine learning has ascended as a pivotal instrument in the domain of drug discovery. Utilizing nonlinear regression, machine learning predictions harness available datasets to disclose inherent patterns. In light of the prevailing data complexity challenges, machine learning-based screening frequently surpasses physics-based methodologies like molecular docking and molecular dynamics (MD) simulations, facilitating a swift screening process of potential drug candidates within expansive chemical libraries. Feng et al. employed machine learning to repurpose compounds from DrugBank targeting MOR, KOR, and DOR, and executed an exhaustive analysis on the binding conformations and drug-likeness of potential drugs with a high predictive binding affinity [25].

In this study, we present a multi-faceted and rigorous strategy that successfully bridges the complex gap between transcriptomic data analysis and drug discovery in the context of substance addiction (Figure 1). We have utilized PST to conduct a topological differentiation of the PPI network derived from DEG data. This innovative approach provides a powerful tool for identifying key genes implicated in opioid and cocaine addiction. The application of PST in our study brings several significant advantages: it facilitates a

multiscale analysis through an intricate filtration process, quantitatively assesses the confidence or strength of each interaction, and extracts high-dimensional information from the PPI network. These features are instrumental in capturing the complex dynamics and interactions within the network, thus providing a more comprehensive understanding of the underlying biological mechanisms. Following a rigorous validation through literature review, pathway analysis, and data-availability scrutiny, we identify three targets highly pertinent to substance addiction: mTOR, mGluR5, and NMDAR for DrugBank repurposing. We devised machine learning (ML) models employing two natural language processing (NLP)-based embeddings generated via transformer and autoencoder models, alongside a traditional 2D fingerprint Extended Connectivity Fingerprint (ECFP). These models demonstrated robust predictive capacity in five-fold cross-validation tests. Leveraging these ML models, we conducted a systematic evaluation of the binding affinities of DrugBank compounds to these targets across various binding thresholds. This examination led to the identification of several drugs exhibiting satisfactory binding energies at specified binding affinity thresholds. Subsequently, molecular docking was performed on a select group of promising drugs to elucidate their interactions with receptors. Additionally, we have conducted a thorough ADMET (absorption, distribution, metabolism, excretion, and toxicity) analysis, providing a comprehensive evaluation of the pharmacokinetic and safety profiles of potential therapeutic compounds. The drugs identified, with their potent receptor inhibition affinities and favorable ADMET profiles, are prime candidates for subsequent biological experiment. This study establishes a new paradigm in drug repurposing research for addiction treatment, seamlessly integrating bioinformatics, topological data analysis, and machine learning into an inclusive and systematic analytical framework. The adaptability of this framework to a wide range of diseases and transcriptomic datasets highlights its potential to significantly advance drug discovery across multiple medical fields.

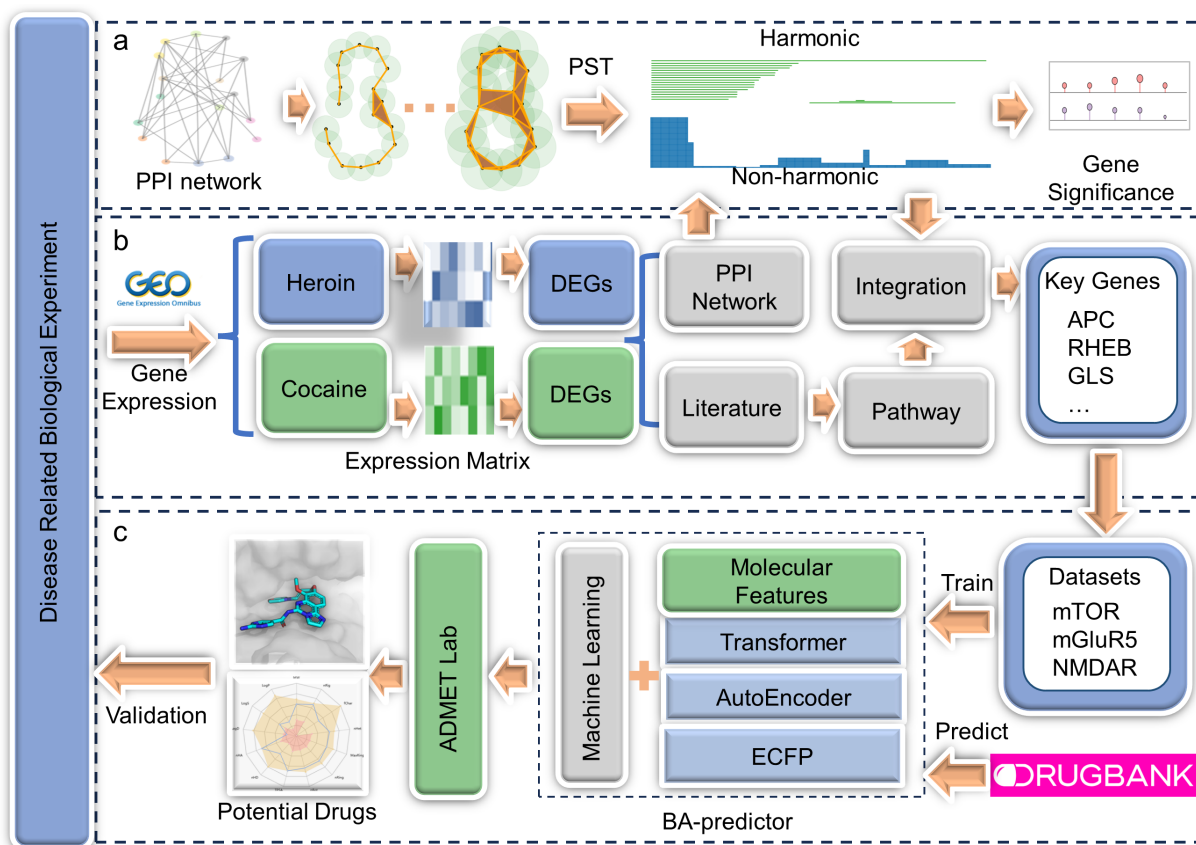


Figure 1: Overview of the Study: (a) PST-Based Topological Differentiation Analysis: This stage involves applying PST for topological differentiation analysis of the PPI network. The method quantifies the significance of nodes within the network in a multiscale manner. (b) DEG Analysis: We extracted opioid and cocaine addiction-related transcriptomic data from the GEO database. Key genes were identified from the PPI network derived from DEGs using topological analysis, and results were integrated across networks with various thresholds. Literature validation and pathway analysis were conducted to confirm the functionality and biological mechanisms of the key genes in substance addiction. (c) Drug Repurposing: Machine learning models, incorporating NLP-based fingerprints and traditional 2D fingerprints, were developed to predict the binding affinities of DrugBank compounds to three addiction-related targets: mTOR, mGluR5, and NMDAR. This process aims to identify potential repurposing candidates after the ADMET analysis for treating substance addiction.

2 Results and Discussion

2.1 Opioid Addiction Analysis

2.1.1 Differential expression analysis

We obtained the GSE87823 dataset from the Gene Expression Omnibus (GEO) database to investigate the gene expression alterations associated with opioid addiction. This dataset encompasses expression data from the human nucleus accumbens, comparing heroin users with controls. The nucleus accumbens is pivotal in regulating reward, emotion, motivation, and goal-directed behavior, making it a focal point for studies on addiction [26]. Heroin, chemically known as 3,6-diacetylmorphine or diamorphine, is a semi-synthetic morphine derivative. It was first synthesized in 1874 and later introduced commercially as a remedy for cough and certain respiratory diseases [27]. However, its potent analgesic effects soon overshadowed its therapeutic uses when it was discovered that heroin could induce intense dependence, leading to illicit consumption [28]. As a result, heroin rapidly became a significant public health concern. Today, it stands as the predominant opioid of abuse in many countries [29]. Intriguingly, despite its widespread

misuse, the psychopharmacology of heroin remains less explored than that of other drugs of abuse, such as cocaine and general psychostimulants [29].

We discerned a total of 295 DEGs in our study: 124 were up-regulated, while 171 were down-regulated (Figure 2a). This distinction provides us with an initial glimpse into the potential molecular mechanisms underlying opioid addiction, as genes that are differentially expressed can hint at pathways and processes that are altered in the disease state.

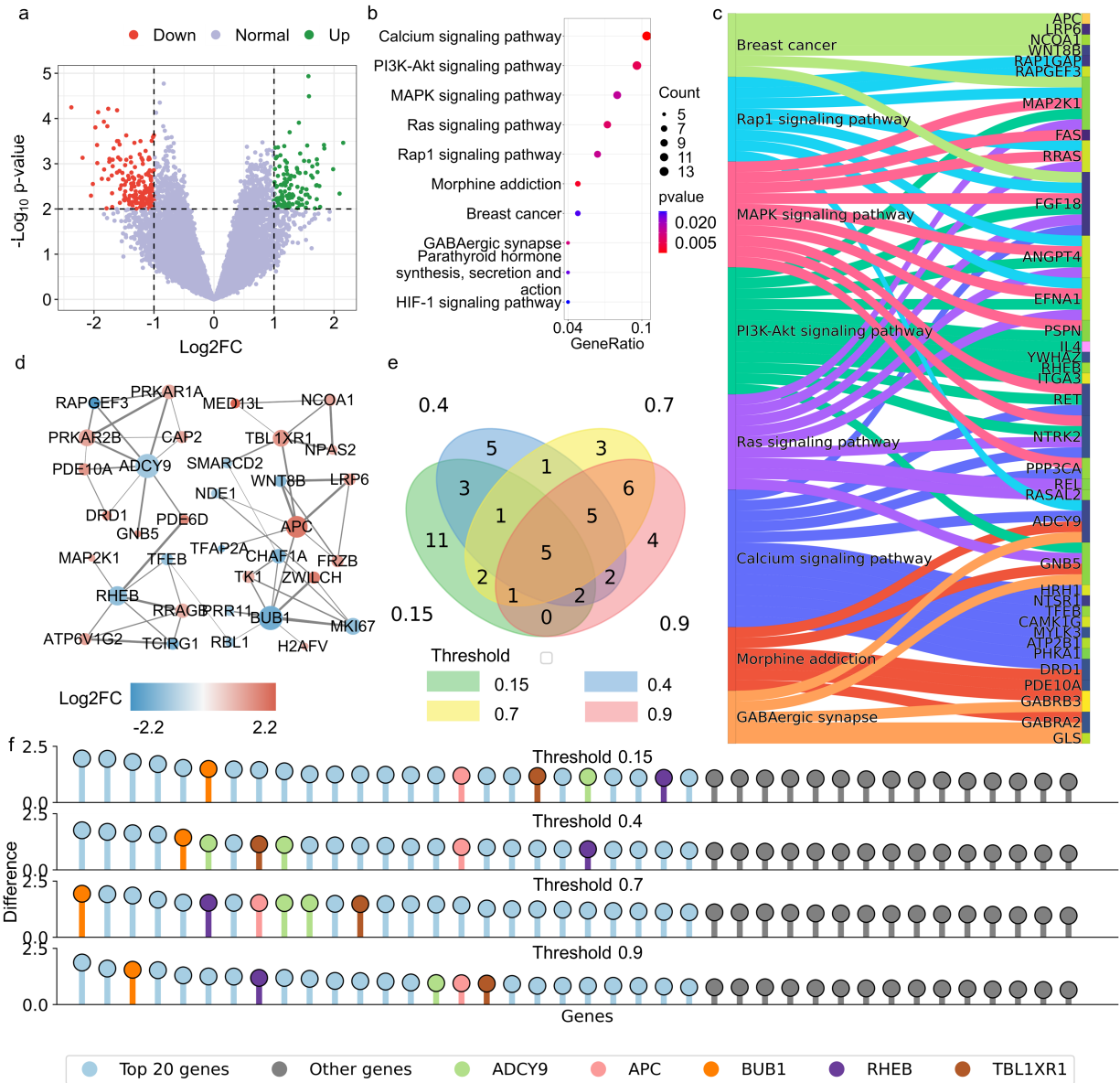


Figure 2: DEG analysis for opioid addiction. (a) Volcano plot of DEGs: This plot visually distinguishes DEGs in opioid addiction, highlighting significant genes above the threshold lines. (b) Enriched pathways in opioid addiction: Showcases the top ten pathways significantly enriched in the context of opioid addiction, emphasizing their relevance in the disease mechanism. (c) Sankey plot of pathway-DEG relationships: Illustrates the top eight enriched pathways and their connections with DEGs, highlighting the intricate interplay between them. (d) Key gene-related PPI sub-network: Depicts the PPI sub-network specifically associated with key genes identified in opioid addiction. (e) Venn diagram of significant intersections: Displays intersections of the top 25 significant genes across four PPI networks with varying thresholds, demonstrating the consistency of key genes in opioid addiction. (f) PST-based network differentiation significance: This graph presents the significance of individual genes as calculated from the PST-based differentiation of the network. For clarity, only the first 40 genes are included.

2.1.2 Multiscale topological differentiation of PPI networks

To further investigate the potential functional interactions among these DEGs, and to pinpoint those that may act as hubs or central players, we retrieved the PPI network for these DEGs from the STRING database (Figure 2b). STRING, a comprehensive database, provides known and predicted protein associations, derived from computational prediction, knowledge transfer between organisms, and interactions aggregated from other databases [30]. By establishing various interaction confidence thresholds (0.15, 0.4, 0.7, and 0.9), we facilitated a multi-resolution analysis. These thresholds enable us to identify robust interactions while also allowing for potential weaker, yet biologically relevant, interactions to be captured.

At the core of our analytical framework is the novel method we termed “multiscale topological differentiation of networks.” As depicted in Figure 3, this method can leverage persistent spectral theory and persistent homology to provide a multidimensional analysis of the network’s topological and geometric characteristics. By constructing a simplicial complex through a carefully designed filtration process, our approach vividly captures the dynamic interplay of protein interactions across various scales.

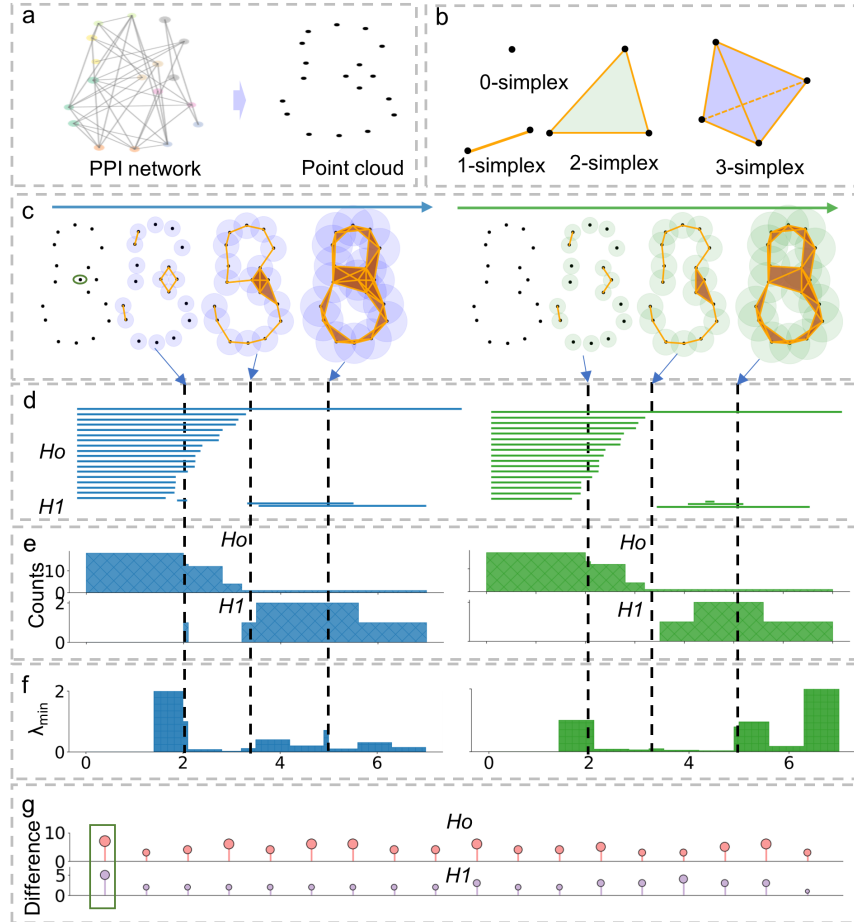


Figure 3: Topological differentiation of network. (a) PPI network as a point cloud: This panel visualizes the PPI network abstracted as a point cloud, forming the basis of a simplicial complex. (b) Basic unit of simplicial complex. (c) Filtration process: This panel depicts the filtration process, which generates a series of simplicial complexes with increasing radii. The left figure shows the original PPI network's simplicial complex, while the right figure displays the new simplicial complex formed after deleting a protein (indicated by the green circle). PH and PST are used to characterize topological and geometric changes post-deletion. (d) Persistent barcodes in topological representation: PH is utilized here to provide a topological representation of the network, illustrated through persistent barcodes. (e) PST is applied to analyze the spectra of persistent Laplacians, with harmonic spectra indicating topological persistence, akin to PH. The figure shows changes in the count of topological invariants during filtration. (f) Capturing homotopic shape Evolution: The non-harmonic spectra in PST highlight the homotopic shape evolution of data. This panel demonstrates the change in the minimum of non-harmonic spectra during the filtration process. (g) Impact of node deletion on topological invariants: This figure illustrates the changes in topological invariants resulting from the deletion of each node in the network. The sum of changes during filtration is shown, with the green rectangle highlighting the changes corresponding to the most significant node.

A key aspect of our methodology is the quantitative nature of the filtration process, based on the distance between proteins, derived from the confidence scores of each interaction pair. This precise and measurable analysis is a fundamental departure from conventional methods predominantly based on centrality algorithms, which often overlook such quantitative interaction information. Our technique exemplifies the application of TDA, effectively tracking the evolution of topological invariants while accounting for changes in homotopic shapes. Our methodology is characterized by its dynamic exploration of the network structure. By systematically removing specific proteins and observing the resulting topological and geometric shifts, we assess the network's structural robustness and the critical role of individual proteins. This analysis allows us to identify key proteins whose modification significantly impacts the network's overall structure.

In this study, we employ PST to meticulously analyze the spectra of persistent Laplacians for each net-

work. This analysis involves a detailed extraction of topological persistence from the harmonic spectra, complemented by insights into the homotopic shape evolution gleaned from the non-harmonic spectra. We then vectorize these extracted features, creating a comprehensive representation of the network's topological characteristics. We calculate the Euclidean distance between vectorized features before and after the deletion of a protein. This distance serves as a metric for assessing the structural impact of the protein's absence, thereby quantifying the protein's importance within the network. Further enhancing our method's precision, we rank the nodes in each network based on their importance under various threshold settings. By identifying and intersecting the top-ranked protein nodes across all four threshold-defined networks, we pinpoint key genes. This intersection approach ensures that the genes we classify as 'key' are consistently influential across multiple network scales, highlighting their potential critical role in the substance addiction related biological processes under study. Applying this methodology, we have successfully identified six key genes that hold significant importance across the networks: APC, BUB1, ADCY9, RHEB and TBL1XR1 (Figure 2e and 2f). Their consistent presence across different network thresholds underscores their potential central role in addiction-related biological pathways.

2.1.3 Literature validation

To gain deeper insights into the intricate relationship between our identified key genes and opioid addiction, we turned to literature validation. Our findings emphasize the significant roles of RHEB, ADCY9, APC, and TBL1XR1 in opioid addiction pathways. RHEB interacts with the mTORC1 pathway, implicating its role in opioid tolerance and hyperalgesia, and suggesting mTOR inhibitors as potential therapeutic agents. ADCY9, pivotal in the cAMP-PKA-GABA pathway, affects neuronal excitability and dopamine release, crucial in addiction mechanisms. APC, through its involvement in the Wnt pathway, is linked to opioid withdrawal symptoms and hyperalgesia. Lastly, TBL1XR1, while less explored, shows potential relevance to opioid addiction via the Wnt pathway. These genes illustrate the multifaceted molecular dynamics of opioid addiction. For more detailed information and literature references, please refer to the supporting information.

2.1.4 Pathway enrichment

To gain a deeper insight into the broader biological processes influenced by the DEGs and to pinpoint significant biological pathways, we conducted pathway enrichment analysis. Figure 2c and 2d depict the top ten enriched signaling pathways. Notably, the three most prominent pathways are the Calcium signaling, PI3K-Akt pathway, and MAPK pathway, involving 13, 12, and 10 DEGs, respectively. Notably, six DEGs have been identified in Morphine addiction pathway.

The intricate link between opioid addiction and calcium signaling has been extensively researched. Upon ligand binding to the opioid receptor, there is a resultant dissociation of the α -GTP complex from the γ dimer subunits. This γ dimer subsequently acts to directly inhibit the calcium channels, leading to a reduction in the intracellular calcium concentration [31]. The modulatory effect of opioid receptor activation on calcium channel activity has been corroborated across various brain regions, including the hippocampus, nucleus locus coeruleus, and the area postrema, among others [32]. König et al. found that PI3K γ modulates the desensitization of the mu opioid receptor [33]. Madishetti et al. discovered the essential function of PI3K γ in cAMP-mediated inflammatory hypernociception [34]. The Mitogen-Activated Protein Kinase (MAPK) pathway is closely associated with opioid addiction. Several genes within MAPK pathway have been identified in relation to opioid receptor signaling and behavior, including ERK 1/2 [35], c-Jun N-terminal kinase [36] and p38 MAPK [37].

2.2 Cocaine Addiction Analysis

2.2.1 Differential expression analysis and key genes identification

We procured and analyzed the GSE54839 dataset from the GEO database to scrutinize the alterations in gene expression consequential to cocaine addiction [38]. This dataset incorporates expression data derived from the human midbrain of chronic cocaine users ($n = 10$) juxtaposed against well-matched drug-free controls ($n = 10$). The midbrain, particularly the dopamine (DA)-synthesizing neurons therein, stands central to our study due to its pivotal role in addiction pathways. These neurons are largely implicated in mediating reward and pleasure centers in the brain, thereby making it crucial to discern the molecular perturbations induced by drug use, specifically in this neural locale. We discerned a total of 824 DEGs. Breaking down this data further revealed 467 up-regulated genes, indicating potential hyperactivity or over-expression in certain pathways, while 356 genes were observed to be down-regulated, signifying possible suppression or reduced activity (Figure 4a). To decipher the potential interplay between these DEGs, we consulted the STRING database to draw their PPI network (Figure 4d). Borrowing from our methodology deployed in the opioid addiction analysis, we leveraged PST to do topological differentiation analysis to identify key genes. These tools, with their distinct mechanisms, enabled us to spotlight pivotal genes within the network. Our differentiation analysis, which spanned multiple confidence thresholds, converged on seven key genes: DNM1, FOS, IL6, JUN, SNAP25, SNCA and SYT1 (Figure 4e and 4f).

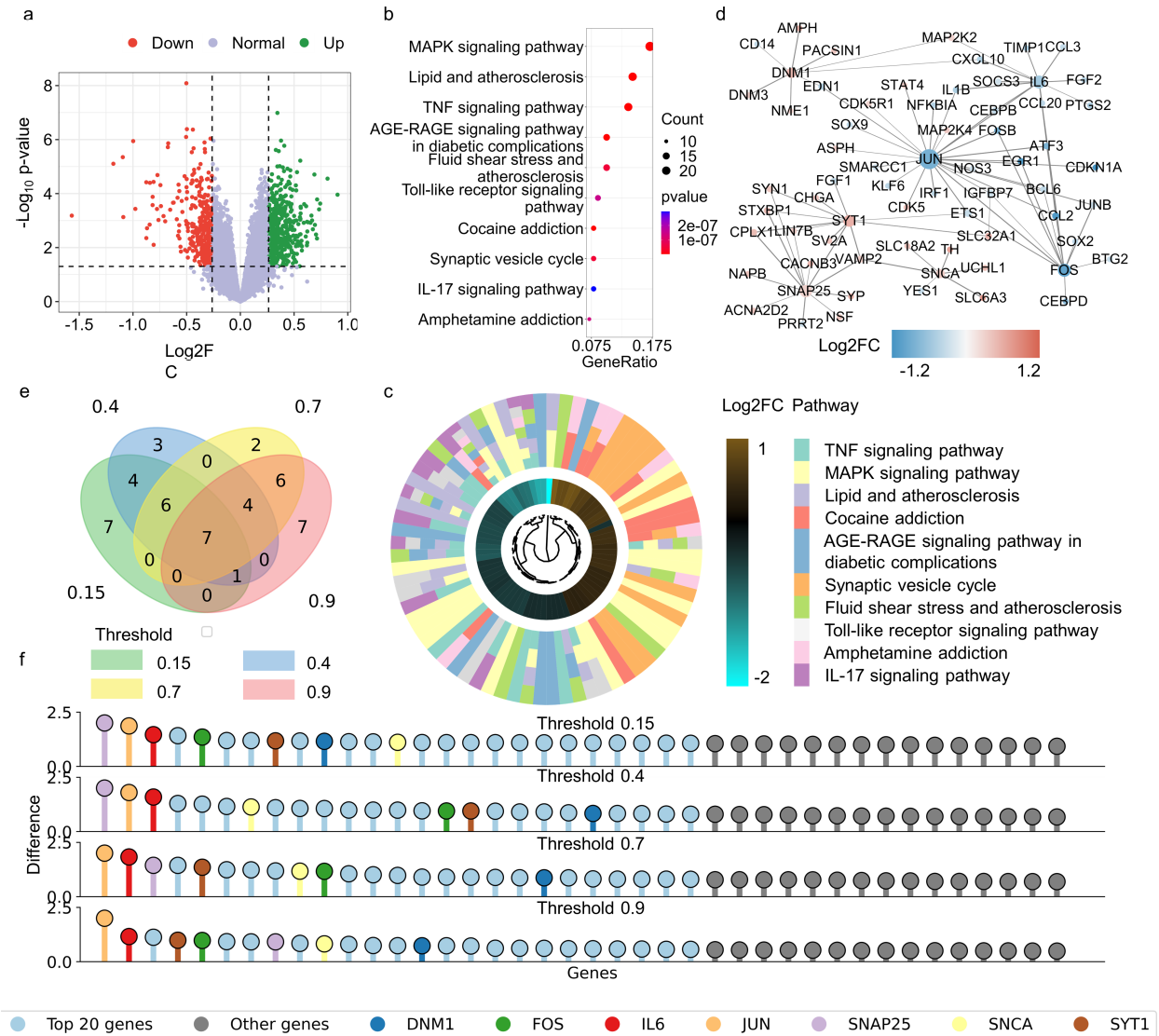


Figure 4: DEG analysis for cocaine addiction. (a) Volcano plot of DEGs: This plot visually distinguishes DEGs in cocaine addiction, highlighting significant genes above the threshold lines. (b,c) Enriched pathways in cocaine addiction: Showcases the top ten pathways significantly enriched in the context of cocaine addiction, emphasizing their relevance in the disease mechanism. (d) Key gene-related PPI sub-network: Depicts the PPI sub-network specifically associated with key genes identified in cocaine addiction. (e) Venn diagram of significant intersections: Displays intersections of the top 25 significant genes across four PPI networks with varying thresholds, demonstrating the consistency of key genes in cocaine addiction. (f) PST-based network differentiation significance: This graph presents the significance of individual genes as calculated from the PST-based differentiation of the network. For clarity, only the first 40 genes are included.

2.2.2 Literature validation

To unravel the intricate interplay between key genes and cocaine addiction, we conducted literature validation. FOS (c-Fos), a significant gene in cocaine addiction, influences neuroplasticity and behavioral responses. Studies reveal that Fos's absence alters the expression of critical neuroadaptation markers and reduces behavioral sensitization to cocaine. Interleukin-6 (IL-6) shows a potential protective effect against cocaine-induced reactions, though evidence remains limited, indicating a need for further research. SYT1 has been linked to cognitive performance in cocaine addiction, with significant associations found between SYT1-rs2251214 and cocaine use disorder (CUD) vulnerability and severity. Lastly, α -synuclein (SNCA) is

recognized for its role in dopaminergic transmission and addictive behaviors. Chronic cocaine abuse leads to an upregulation of SNCA, with implications extending to other substances like alcohol. This validation underscores the complexity of genetic influences in cocaine addiction. For more comprehensive details and references, please refer to the supporting information.

2.2.3 Pathway enrichment

In an effort to elucidate the underlying biological processes linked to cocaine addiction, we undertook a comprehensive pathway enrichment analysis. The results, as illustrated in Figure 4b and 4c, highlight the ten most significant signaling pathways associated with this condition. Notably, the Cocaine and Amphetamine addiction pathways emerge as direct correlates to substance dependency. At the forefront of these pathways are the MAPK signaling cascade, the Lipid metabolism and atherosclerosis pathway, and the TNF signaling axis. It is of particular significance that the MAPK signaling cascade, previously implicated in opioid addiction studies, reemerges here, accentuating its pivotal role in the broader context of substance addiction [39,40].

The association of cocaine with the Lipid metabolism and atherosclerosis pathway underscores the drug's deleterious cardiovascular implications. Many studies have documented the profound vascular influence of cocaine intake, emphasizing inflammation and atherosclerosis as predominant systemic outcomes with both acute and chronic manifestations [41, 42]. Not much literature evidence of relations between TNF signaling pathway and cocaine addiction was found. The only exception was due to Lewitus et al. who demonstrated that microglial TNF- α can modulate cocaine-induced neural plasticity and behavioral sensitization [43].

2.3 Integrated Analysis of Opioid and Cocaine Addiction DEGs

In our endeavor to unravel the shared molecular mechanisms underlying opioid and cocaine addiction, we integrated the DEGs identified in both conditions. Our primary goal was to pinpoint key genes that are consistently involved in both types of drug addictions. These genes could serve as potential therapeutic targets or biomarkers, crucial for the treatment and diagnosis of addiction. Utilizing our sophisticated topological differentiation analysis, we were able to identify eight central genes that play significant roles across both addiction types: RHEB, DNMI, FOS, IL1B, IL6, JUN, SNAP25, and SNCA (5a). Notably, IL1B emerged as a novel target, a gene not previously associated with either opioid or cocaine addiction in existing analyses. In contrast, RHEB was previously recognized in the opioid addiction DEG PPI network, underscoring its importance in opioid-related mechanisms. The remaining six genes - DNMI, FOS, IL6, JUN, SNAP25, and SNCA - were identified through our analysis of cocaine addiction. Consistent with earlier studies, we conducted a pathway enrichment analysis on the integrated genes derived from both opioid and cocaine addiction analyses. As anticipated, the MAPK signaling pathway emerged as a top-ranking pathway, underscoring its crucial role in substance addiction. Figure 4b presents the top ten pathways identified, highlighting the prominence of the MAPK pathway among them.

We then adopted a more streamlined strategy, focusing explicitly on genes that were consistently differentially expressed in both opioid and cocaine addictions. This approach revealed ten genes: CAMK1G, GABRB3, ACOT7, CAP2, PTPRN2, RET, GLS, NTRK2, BLZF1, and RAP1GAP. Most notably, seven out of these ten genes (CAMK1G, GABRB3, ACOT7, CAP2, PTPRN2, RET, and GLS) exhibited parallel expression deviations in both addiction conditions. This consistent pattern accentuates the potential significance of these genes in the broader context of drug addiction and may suggest a shared molecular pathway influencing the pathophysiology of both opioid and cocaine addictions Figure (5c).

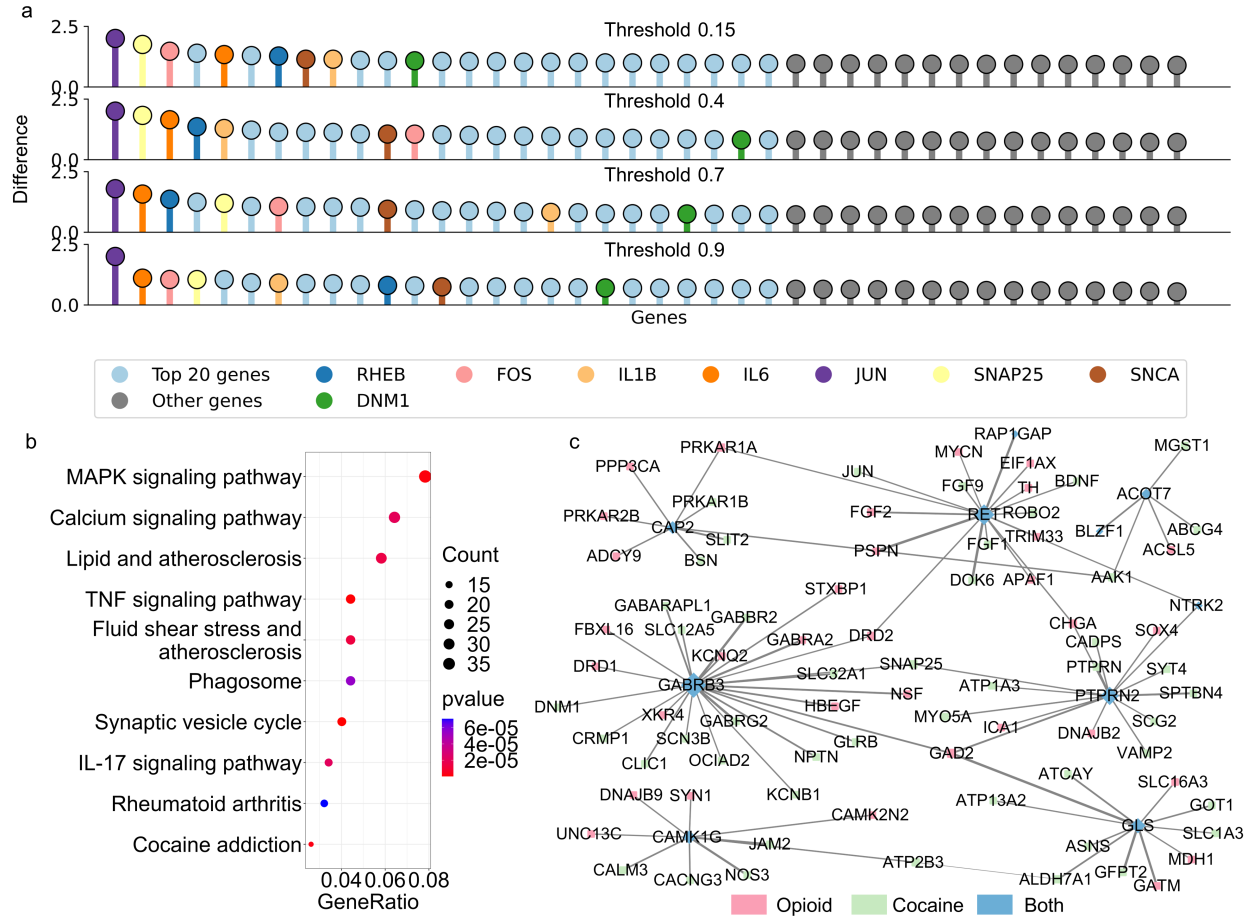


Figure 5: Integrated analysis of opioid and cocaine addiction DEGs. (a) PST-based network differentiation significance: This graph displays the significance of individual genes as determined by the PST-based differentiation in the integrated network of opioid and cocaine addiction DEGs. To enhance clarity, only the first 40 genes are shown. (b) Enriched pathways in integrated DEGs: Illustrates the pathways that are significantly enriched in the context of the integrated DEGs from both opioid and cocaine addiction, highlighting their combined biological relevance. (c) PPI sub-network related to common DEGs: Depicts the PPI sub-network associated with DEGs that are present in both opioid and cocaine addiction conditions, emphasizing the shared molecular mechanism.

2.3.1 Literature validation

Extensive literature validation reveals a significant association between *GABRB3*, *PTPRN2*, *GLS*, and *IL1B* genes and drug addiction. *GABRB3*, encoding the β_3 subunit of the GABAA receptor, is implicated in heroin dependence and alcoholism, with studies suggesting its key role in addiction pathogenesis. *PTPRN2*, linked to substance dependence and cognitive behavior, shows relevance in cocaine dependence and depression comorbidity, and its knockout mice models indicate altered neurotransmitter concentrations. Glutaminase (*GLS*), crucial in glutamate production, emerges as a central enzyme in drug reward mechanisms and relapse propensity due to its regulation of excitatory neurotransmission. Finally, *IL1B*, associated with inflammatory responses to cocaine, shows genetic links to alcohol and opioid dependence, highlighting its potential as a biomarker or therapeutic target in addiction. These findings illustrate the complex genetic underpinnings of addiction and underscore the cross-substance implications of these genes. For a detailed exploration of these associations and references, please refer to the supporting information.

2.4 Repurposing of DrugBank for addiction-related targets

2.4.1 Binding affinity predictors for addiction-related targets

To advance the therapeutic treatment of drug addiction and unearth potential therapeutic agents, we employed machine learning techniques to repurpose drugs from DrugBank. Machine learning models, given their ability to discern patterns and relationships in vast datasets, can effectively predict how various drugs might interact with specific biological targets associated with addiction. However, the success of these models hinges on access to a rich dataset of compound activities. Our initial search in the ChEMBL database for compounds related to our literature-validated key genes revealed a data insufficiency, precluding effective model development. This challenge redirected our focus to proteins that function downstream of these key genes. From our investigation, three proteins with substantial inhibitor data were identified: mTOR, NMDAR, and mGluR5. As we had previously deduced, RHEB’s association with opioid addiction likely operates via the mTORC1 pathway. With respect to GLS, the impact on neuronal excitability from its product, glutamate, is majorly steered by NMDAR and mGluR5. Their profound connection to substance addiction has been corroborated by numerous studies [44–47].

We identified 4,392 mTOR inhibitors, 1,777 for mGlu5, and 2,342 for NMDAR, all characterized by either IC_{50} or K_i data in ChEMBL. Given the intricate nature of molecular structures, accurately representing them for machine learning models is a non-trivial task. We adopted a multi-pronged approach to molecular representation, employing both deep learning and traditional molecular fingerprint techniques. Specifically, we utilized transformer-based architectures, sequence-to-sequence autoencoders, and the established ECFP to capture the nuanced structural features of these molecules. These representations were then used to train Gradient Boosted Decision Trees (GBDT), a robust machine learning algorithm, to predict the inhibitory activities of the molecules on our target proteins. In order to offer a more robust and reliable prediction by capitalizing on the strengths of individual models, we constructed a consensus model for each target. Our model yielded Pearson correlation coefficients (R) of 0.876, 0.754, and 0.799 for mTOR, mGlu5, and NMDAR, respectively. In terms of prediction accuracy, the root mean square errors (RMSE) were found to be 0.758, 0.882, and 0.991, respectively.

2.4.2 Potential inhibitors of addiction-related targets in DrugBank

To discover potential inhibitors targeting addiction-related proteins, we deployed our machine learning predictors to gauge the binding affinity of various small molecules housed in the DrugBank database. DrugBank classifies small molecules into diverse states based on their clinical statuses. For the scope of our research, we narrowed our focus exclusively on two key categories: ‘approved’ and ‘investigational’. These categories are of particular interest as they encompass molecules that have either received regulatory approval or are currently under investigation in clinical studies, implying a higher likelihood of therapeutic potential and translational relevance in the context of addiction. In our analysis, we specifically selected molecules exhibiting a binding affinity greater than -9.54 kcal/mol (equivalent to a K_i value of 100 nM). Such a stringent criterion, widely recognized in drug discovery, ensures that we consider only those compounds with a significant potential for therapeutic action [48].

2.4.2.1 Approved drugs with predicted efficacy on mTOR We embarked on an evaluation of approved drugs that demonstrated strong binding affinity towards mTOR, with our selected affinity thresholds set at -11 kcal/mol, -10 kcal/mol, and -9.54 kcal/mol. In accordance with these thresholds, we identified 4, 7, and 7 drugs, respectively, that matched our criteria (Table 1).

Table 1: Summary of the FDA-approved drugs that are potential potent inhibitors of mTOR with binding affinity (BA) \leq -9.54 kcal/mol.

DrugID	Name	Predicted BA (kcal/mol)
DB00877	Sirolimus	-12.46
DB00864	Tacrolimus	-12.32
DB01590	Everolimus	-12.07
DB00337	Pimecrolimus	-11.39
DB12483	Copanlisib	-10.40
DB11943	Delafloxacin	-10.31
DB09272	Eluxadoline	-10.31
DB01764	Dalfopristin	-10.12
DB00705	Delavirdine	-10.07
DB00709	Lamivudine	-10.05
DB00615	Rifabutin	-10.04
DB00879	Emtricitabine	-9.92
DB00210	Adapalene	-9.91
DB12153	Citicoline	-9.87
DB12767	Gaxilose	-9.84
DB13274	Micronomicin	-9.72
DB06725	Lornoxicam	-9.61
DB08907	Canagliflozin	-9.59

Of particular note, both Sirolimus and Everolimus are known mTOR inhibitors [49, 50]. Sirolimus, also known as Rapamycin, was the first pharmacological agent developed in the class of mTOR inhibitors. It received FDA approval in 1999 to deter transplant rejection in kidney recipients. It is synthesized by the bacterium *Streptomyces hygroscopicus* and is characterized as a macrocyclic lactone antibiotic. Apart from its primary indication, it is also utilized to manage lymphangiomyomatosis. In the US, a specific formulation of Sirolimus, albumin-bound Sirolimus for intravenous administration, has been indicated for treating adult patients with advanced unresectable or metastatic malignant perivascular epithelioid cell tumors (PEComa). On the other hand, Everolimus shares a functional similarity with Sirolimus in inhibiting mTOR but possesses a more favorable pharmacokinetic profile, featuring greater bioavailability, a more rapid terminal half-life, and distinct blood metabolite patterns. The FDA has approved Everolimus to prevent rejection after solid organ transplants and for treating a range of tumors, including breast, renal, and neuroendocrine tumors. Tacrolimus and Pimecrolimus are both calcineurin inhibitors, and, similar to sirolimus, they possess a macrocyclic lactone structure. Tacrolimus is primarily utilized as an immunosuppressant following kidney transplantation and is also indicated for treating atopic dermatitis when applied topically. Conversely, Pimecrolimus is specifically formulated as a topical agent for the management of mild to moderate atopic dermatitis (eczema) in patients who either do not respond well to or cannot tolerate other treatments, such as topical steroids.

Copanlisib is prescribed for adults with recurrent follicular lymphoma, particularly those who have already received a minimum of two prior treatments. It is categorized as a phosphoinositide 3-kinase (PI3K) inhibitor, exhibiting selective inhibition towards the alpha and delta isoforms of PI3K found in malignant B-cells [51]. Delafloxacin is a fluoroquinolone antibiotic used to treat specific bacterial infections in adults, such as skin infections and some pneumonias [52, 53]. It works by eliminating bacteria or inhibiting their growth, and is indicated for acute bacterial skin and skin structure infections (ABSSSI) and community-acquired bacterial pneumonia (CABP) caused by susceptible bacteria. Eluxadoline is prescribed to treat irritable bowel syndrome with diarrhea (IBS-D) in adults [54]. It acts as an agonist on mu and kappa opioid receptors and an antagonist on delta opioid receptors. This modulation reduces bowel activity, stabilizes

intestinal contractility, and balances stress-induced acceleration in the upper GI tract, alleviating IBS-D symptoms.

To gain a more detailed insight into how these drugs might exert inhibitory effects on mTOR, we embarked on molecular docking analysis. This approach aimed to unveil the nuances of their binding modes and their specific interactions with the mTOR protein. As illustrated in Figure 6, Copanlisib, Delafloxacin, and Eluxadoline exhibit distinctive yet overlapping binding patterns to mTOR. One of the common characteristics among these drugs is their interaction with Thr2245. All three molecules establish hydrogen bonds with this residue: Copanlisib and Eluxadoline leverage their oxygen atoms for this interaction, while Delafloxacin utilizes its nitrogen atom. Additionally, both Copanlisib and Delafloxacin form hydrogen bonds with Val2240, but they achieve this interaction via their respective oxygen atoms. Digging deeper into their unique interactions, Copanlisib forms an additional hydrogen bond through its nitrogen atom, targeting the side chain hydroxyl group of Ser2342. Conversely, Delafloxacin establishes a connection with the side chain amino group of Lys2187, facilitated by one of its fluorine atoms. On the other hand, Eluxadoline is distinctive in its ability to form hydrogen bonds with both Arg2348 and Ser2165 through its oxygen atoms.

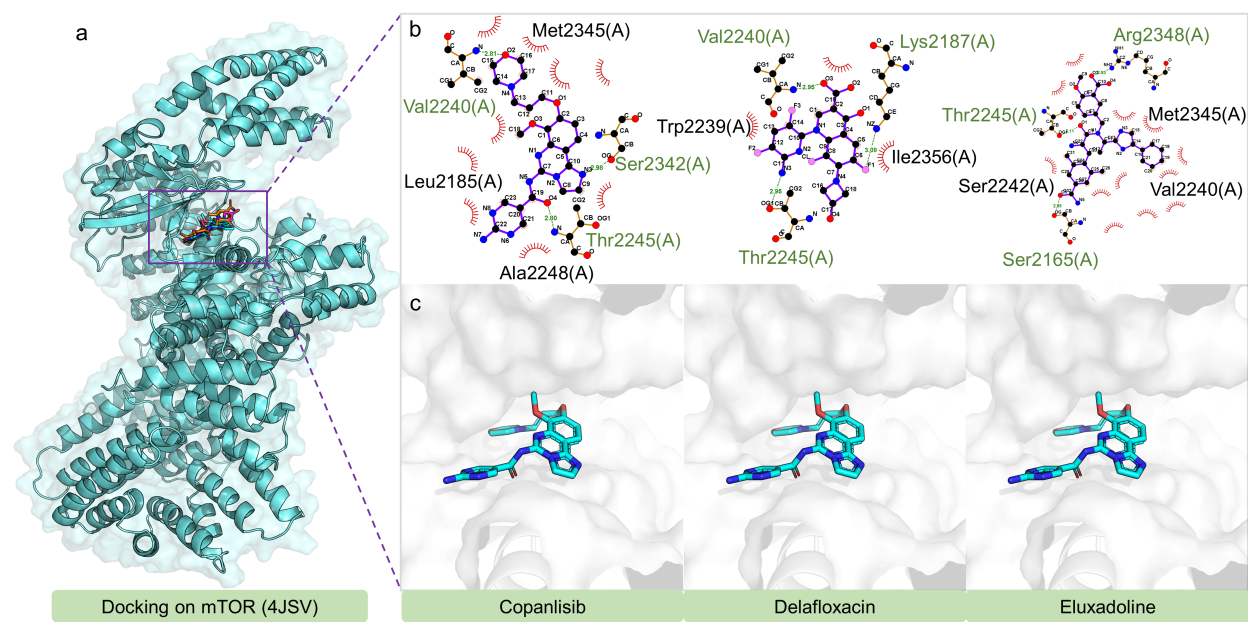


Figure 6: The docking structures and interactions of Copanlisib, Delafloxacin, and Eluxadoline with mTOR.

2.4.2.2 Investigational drugs with predicted efficacy on mTOR In our analysis of investigative drugs for potential efficacy on mTOR, we observed a greater proportion of these drugs exhibiting high affinity compared to approved drugs, as listed in Table 2, which includes only compounds with a binding affinity better than -11 kcal/mol. Notably, while Ridaforolimus specifically targets mTOR [55], the remaining compounds are dual inhibitors of PI3K and mTOR. Omipalisib (GSK2126458 or GSK458) has been investigated for treating various cancers, including acute myeloid leukemia (AML), demonstrating promising anti-leukemia effects [56]. Gedatolisib (PF-05212384 or PKI-587), originally developed by Wyeth, has advanced to clinical trials for diverse cancer types [57, 58], earning FDA fast track designation for certain breast cancer treatments. PKI-179, derived from Gedatolisib, is a dual PI3K and mTOR inhibitor developed primarily for advanced malignant solid tumors [59].

Table 2: Summary of investigational drugs that have the potential to inhibit mTOR.

DrugID	Name	Predicted BA (kcal/mol)
DB12703	Omipalisib	-13.06
DB11896	Gedatolisib	-12.36
DB13109	PKI-179	-12.34
DB11836	Sapanisertib	-12.20
DB12774	AZD-8055	-11.74
DB11925	Vistusertib	-11.50
DB13072	GDC-0349	-11.24
DB06233	Ridaforolimus	-11.21
DB12570	CC-223	-11.01

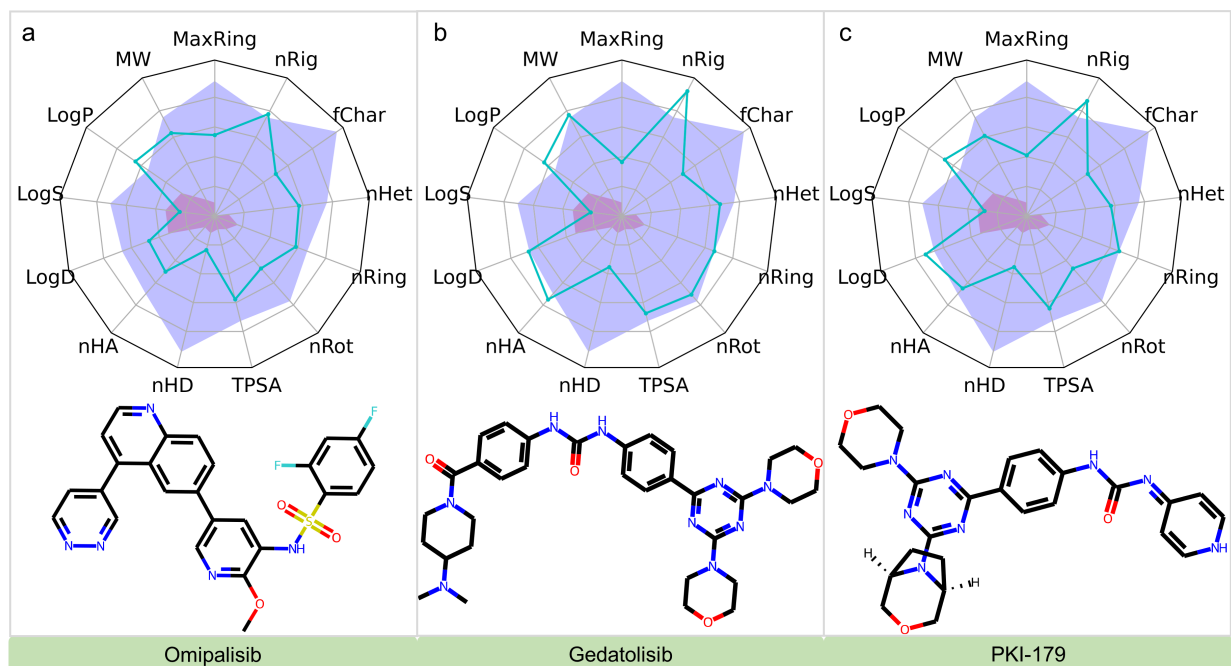


Figure 7: Evaluations of ADMET Properties for Omipalisib, Gedatolisib, and PKI-179: This figure illustrates the ADMET profiles of Omipalisib, Gedatolisib, and PKI-179, with the blue curves representing the values of 13 specified ADMET properties. The yellow and red zones demarcate the upper and lower limits, respectively, of the optimal ranges for these properties. The data shown are predictive results obtained from the ADMETlab 2.0 website (<https://admetmesh.scbdd.com/>). The evaluated ADMET properties include Molecular Weight (MW), the logarithm of the octanol/water partition coefficient (logP), the logarithm of the aqueous solubility (logS), the logP at physiological pH 7.4 (logD), Number of hydrogen bond acceptors (nHA), Number of hydrogen bond donors (nHD), Topological polar surface area (TPSA), Number of rotatable bonds (nRot), Number of rings (nRing), Number of atoms in the biggest ring (MaxRing), Number of heteroatoms (nHet), Formal charge (fChar), and Number of rigid bonds (nRig).

2.4.2.3 Approved drugs with predicted efficacy on mGluR5 In our analysis of DrugBank, we found that fewer approved drugs exhibited a high binding affinity for mGluR5 as compared to mTOR. Specifically, only two drugs, Doravirine and Desogestrel, displayed a binding affinity better than -10 kcal/mol, as detailed in Table 3.

Table 3: Summary of the FDA-approved drugs that are potential potent inhibitors of mGluR5 with BA Δ -9.54 kcal/mol.

DrugID	Name	Predicted BA (kcal/mol)
DB12301	Doravirine	-10.52
DB00304	Desogestrel	-10.05
DB12612	Ozanimod	-9.90
DB01595	Nitrazepam	-9.87
DB06636	Isavuconazonium	-9.85
DB09291	Rolapitant	-9.78
DB08439	Parecoxib	-9.75
DB00294	Etonogestrel	-9.73
DB00475	Chlordiazepoxide	-9.72
DB11633	Isavuconazole	-9.68
DB00404	Alprazolam	-9.65
DB00904	Ondansetron	-9.63
DB15685	Selpercatinib	-9.62
DB11374	Amprolium	-9.57

Doravirine serves as an antiviral agent specifically designed to combat HIV infections. It functions as a non-nucleoside reverse transcriptase inhibitor (NNRTI), targeting the reverse transcriptase enzyme of HIV-1. This enzyme is central to HIV replication, as it synthesizes complementary DNA (cDNA) from the virus’s RNA. Importantly, Doravirine’s mode of action non-competitively inhibits the HIV-1 reverse transcriptase without affecting human cellular DNA polymerases α , β , and mitochondrial DNA polymerase γ [60]. Desogestrel is a synthetic progestin used primarily for contraception, either alone or in combination with an estrogen such as ethinyl estradiol. Its contraceptive efficacy arises mainly from the inhibition of ovulation [61]. Ozanimod, commercially known as Zeposia, is a medication used for the treatment of relapsing forms of multiple sclerosis [62] and ulcerative colitis [63] in adults. Its mechanism of action is centered on modulating the sphingosine-1-phosphate (S1P) receptor. This modulation curtails the proliferation of lymphocytes, which are pivotal in inciting inflammation within the cerebral and gastrointestinal regions.

We performed a detailed exploration of the binding mechanisms of these three drugs with mGluR5, utilizing molecular docking techniques. Figure 8 illustrates the binding poses and intermolecular interactions between Doravirine, Desogestrel, and Ozanimod with the mGluR5 active site. A salient feature observed across all three drug-receptor complexes is the hydrogen bonding interaction with the Thr175 residue. Specifically, Doravirine forms this bond utilizing its oxygen atom, whereas Desogestrel and Ozanimod achieve this interaction through their respective nitrogen atoms. This consistent interaction with Thr175 underscores its potential as a critical residue in modulating drug-target affinity within the mGluR5 receptor. Further interaction analysis revealed that Doravirine establishes an additional hydrogen bond with Asp195. In contrast, Ozanimod predominantly engages via hydrogen bond interactions, interacting notably with Ser151, Ser152, and Gln198. Desogestrel, in its interaction profile, primarily engages in hydrophobic interactions, emphasizing its distinct binding dynamics within the mGluR5 receptor’s active site.

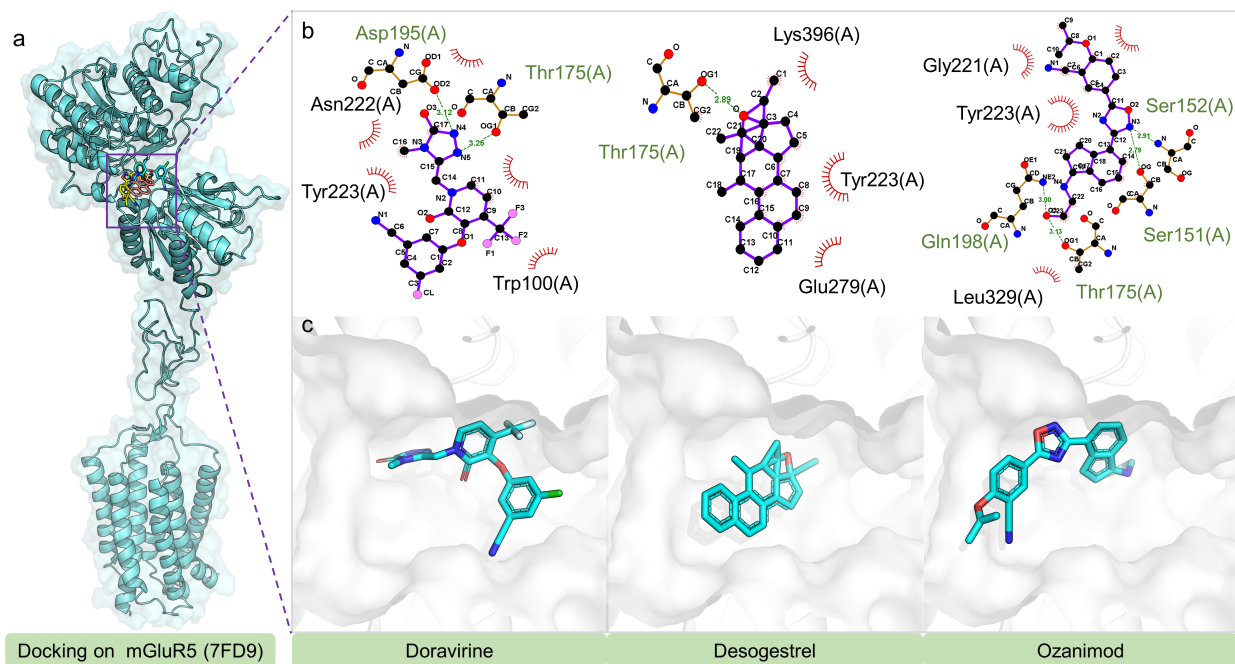


Figure 8: The docking structures and interactions of Doravirine, Desogestrel, and Ozanimod with mGluR5.

2.4.2.4 Investigational drugs with predicted efficacy on mGluR5 In our subsequent analysis, we explored further investigational drugs projected to influence mGluR5 activity. It was observed that a greater number of these investigational drugs exhibited a higher affinity towards mGluR5 compared to approved drugs. Table 4 restrictively lists compounds boasting a binding affinity stronger than -10kcal/mol.

Table 4: Summary of investigational drugs that have the potential to inhibit mGluR5.

DrugID	Name	Predicted BA (kcal/mol)
DB13004	Mavoglurant	-10.88
DB12733	Dipraglurant	-10.82
DB11649	Lersivirine	-10.40
DB12999	MK-6186	-10.17
DB15406	GLPG-0974	-10.11
DB04885	Cilansetron	-10.11
DB14929	Elsulfavirine	-10.10
DB13035	AG-24322	-10.02
DB12931	Fenobam	-10.01

Among these, Mavoglurant and Dipraglurant stand out as mGluR5 antagonists. Mavoglurant's early investigations were centered around its potential treatment for Fragile X syndrome [64], and subsequently, for levodopa-induced dyskinesia (LID) associated with Parkinson's disease (PD) [65]. Unfortunately, its progression to clinical use has been halted due to its inability to achieve primary endpoints in advanced clinical trials. On the other hand, Dipraglurant has been specifically formulated to mitigate LID prevalent in PD patients [66]. Lersivirine (or UK-453061) is a distinct compound from the pyrazole class, emerging as a part of the next-generation NNRTIs. Spearheaded by ViiV Healthcare, its primary purpose was to challenge HIV-1 infection [67].

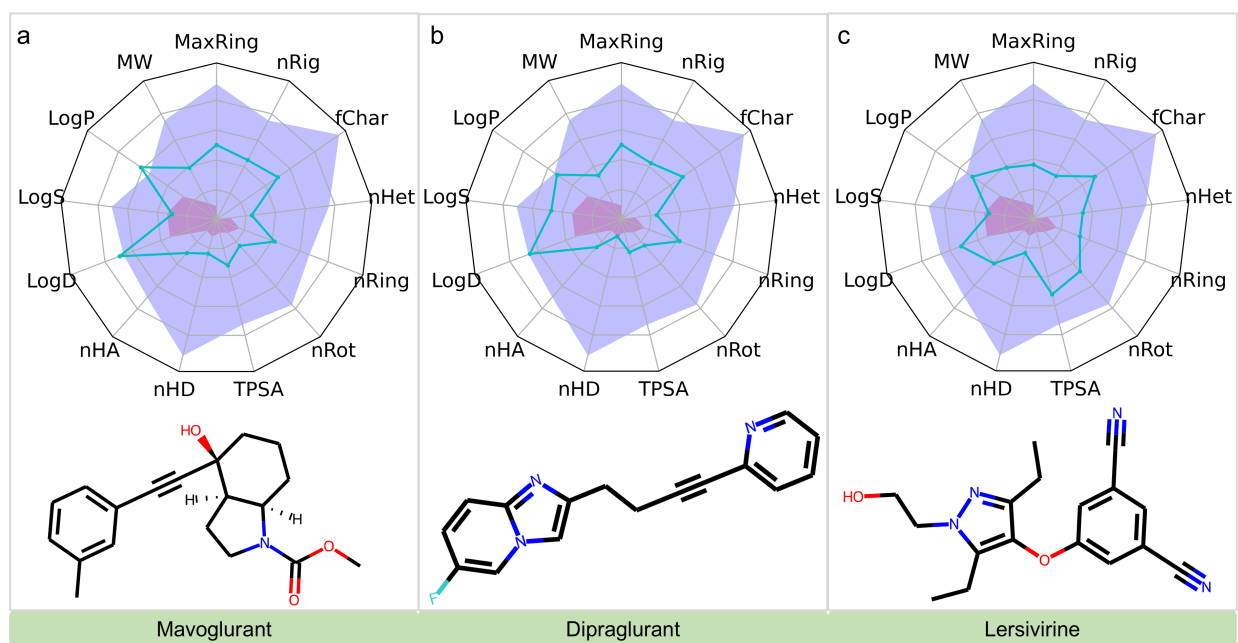


Figure 9: Evaluations of ADMET Properties for Mavoglurant, Dipraglurant, and Lersivirine: This figure showcases the ADMET profiles for Mavoglurant, Dipraglurant, and Lersivirine. The blue curves in the graph indicate the values for 13 specific ADMET properties of these compounds. The yellow and red zones in the graph are designated to highlight the upper and lower limits of the optimal ranges for each of these ADMET properties, respectively.

2.4.2.5 Approved drugs with predicted efficacy on NMDAR In our analysis of DrugBank, we identified only 7 approved drugs that exhibit a binding affinity greater than -9.54 kcal/mol to NMDAR. (Table 5)

Table 5: Summary of the FDA-approved drugs that are potential potent inhibitors of NMDAR with $BA \leq -9.54$ kcal/mol.

DrugID	Name	Predicted BA (kcal/mol)
DB00157	NADH	-10.10
DB03147	FAD	-10.09
DB00705	Delavirdine	-9.75
DB00131	Adenosine phosphate	-9.69
DB00118	Ademetionine	-9.61
DB00364	Sucalfate	-9.56
DB08874	Fidaxomicin	-9.56

Among these, Nicotinamide Adenine Dinucleotide (NADH) and Flavin Adenine Dinucleotide (FAD) stand out as crucial coenzymes that participate in various biochemical reactions within the body. There is some evidence to suggest that NADH could be beneficial in treating conditions such as Parkinson's disease and chronic fatigue syndrome [68]. Delavirdine, marketed under the brand name Rescriptor, is classified as a NNRTI and was developed to treat HIV-1 [69]. It exerts its therapeutic effects by binding directly to the reverse transcriptase enzyme, thereby inhibiting both RNA-dependent and DNA-dependent DNA polymerase activities. Adenosine phosphate is an adenine nucleotide with a single phosphate group. Initially introduced as a vasodilator and anti-inflammatory agent, it faced withdrawal by the FDA due to concerns regarding its safety and efficacy for these indications. Nevertheless, it has found applications in nutritional supplementation and in addressing dietary insufficiencies or imbalances [70]. Ademetionine, commonly referred to as S-adenosylmethionine (SAMe), is a naturally occurring molecule in the body. It serves as a crucial physiological methyl donor, participating in enzymatic transmethylation processes essential to all

living organisms. In the U.S., SAME has been marketed as a dietary supplement, touted for its benefits in supporting mood and emotional well-being [71].

We conducted docking studies of Delavirdine, Adenosine phosphate, and Ademetionine with the active site of NMDAR to elucidate their interaction patterns (Figure 10). Predominantly, these drugs employ hydrophobic interactions for their binding to NMDAR. Notably, all three drugs establish hydrogen-bonding interactions with Thr648. Furthermore, Adenosine phosphate uniquely forms a hydrogen bond with the side chain hydroxyl group of the neighboring residue, Thr647. We did not observe any other significant interaction types in this analysis.

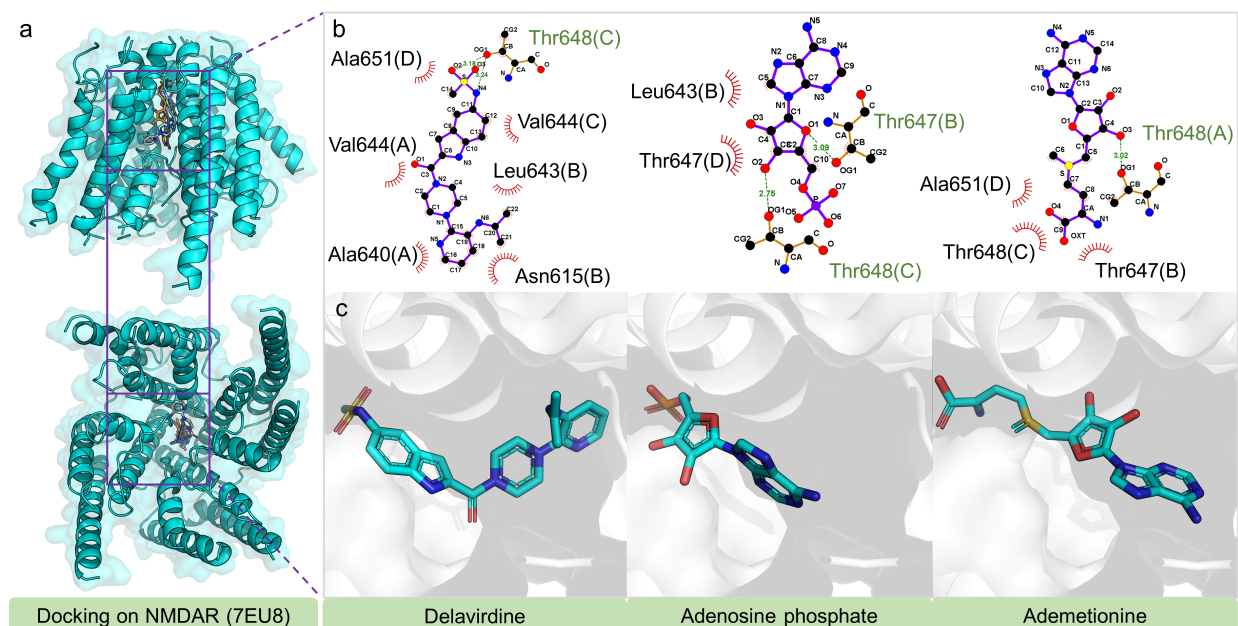


Figure 10: The docking structures and interactions of Delavirdine, Adenosine phosphate, and Ademetionine with NMDAR.

2.4.2.6 Investigational drugs with predicted efficacy on NMDAR In our pursuit to identify potential modulators of NMDAR, we explored further the realm of investigational compounds. Notably, a larger proportion of these compounds exhibited higher affinity for NMDAR in comparison to approved drugs. For brevity, only the top 10 of these compounds are presented in Table 6.

Table 6: Summary of top-10 investigational drugs that have the potential to inhibit NMDAR.

DrugID	Name	Predicted BA (kcal/mol)
DB06741	Gavestinel	-11.70
DB12365	Perzinfotel	-10.84
DB12749	Butylphthalide	-10.47
DB05553	Regrelor	-10.23
DB12140	Dilmapimod	-10.14
DB03708	Adenosine 5'-phosphosulfate	-10.12
DB13019	Henatinib	-9.92
DB06334	Tucidinostat	-9.84
DB12012	PF-04457845	-9.83
DB05973	Inosine 5'-sulfate	-9.79

Among them, Gavestinel and Perzinfotel emerged as notable NMDAR antagonists. Gavestinel was orig-

inally earmarked for the therapeutic management of acute intracerebral hemorrhage. Mechanistically, it operates as a non-competitive antagonist, targeting the glycine binding site on the NMDA receptor. Gavestinel's specificity is underscored by its remarkable selectivity, manifesting over a 1000-fold preference for the NMDA receptor over other receptor binding sites like AMPA and kainate [72]. Beyond its in vitro affinity, Gavestinel also proved to be orally bioavailable with in vivo activity [72]. Perzinfotel, on the other hand, has been the subject of clinical investigations geared towards stroke [73]. Butylphthalide is a chemical constituent isolated from celery oil. Preliminary research, particularly in preclinical models, has hinted at its multifaceted therapeutic potential in hypertension management and neuroprotection [74]. The neuroprotective potential of butylphthalide garnered considerable attention in clinical circles, especially its therapeutic potential against acute ischemic stroke [75].

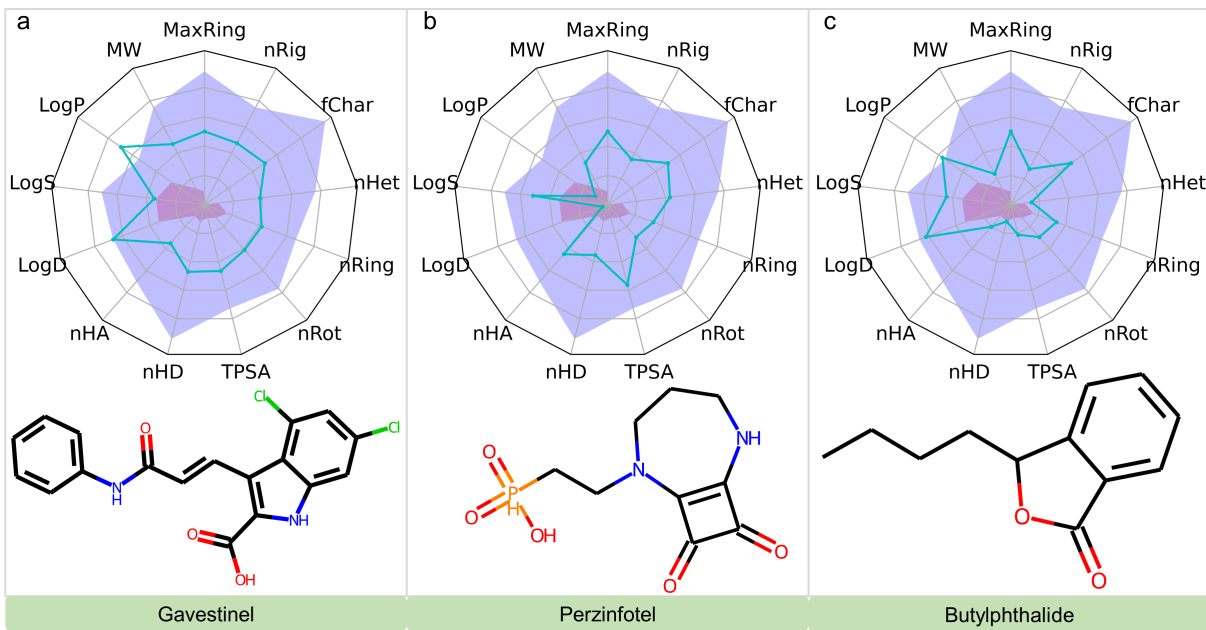


Figure 11: Evaluations of ADMET Properties for Gavestinel, Perzinfotel, and Butylphthalide.

2.4.3 ADMET analysis

Understanding that a molecule's pharmacokinetic and safety profiles are pivotal in its clinical trial success, we focused on the ADMET (absorption, distribution, metabolism, excretion, and toxicity) properties of our identified investigational drugs. A comprehensive understanding of these properties is crucial, as drug candidates can fail in advanced stages if they do not meet ADMET criteria, which govern their behavior within the human body [76]. Utilizing the ADMETlab 2.0 tool, we assessed 13 distinct ADMET attributes for each drug which show potential efficacy on the three targets [76].

For mTOR inhibitors, our analysis revealed that Omipalisib has a logP value slightly exceeding the optimal range, which can potentially affect its solubility and permeability (Figure 7). However, its other ADMET properties fell within acceptable limits, suggesting a favorable pharmacokinetic profile overall. On the other hand, Gedatolisib presented some challenges, with a relatively large molecular weight and a higher number of rings and hydrogen bond donors. These structural features contribute to its high logP value, resulting in poor water solubility. Similarly, while PI3K, developed from Gedatolisib, has a smaller molecular weight, it inherits the challenge of a high logP value and limited water solubility.

In the case of mGluR5 inhibitors (Figure 9), we found that Mavoglurant's logP and logD values surpassed recommended thresholds, indicating potential issues with water solubility. However, its other ADMET

properties were within acceptable ranges. Dipraglurant and Lersivirine, on the other hand, showed well-balanced ADMET profiles, suggesting favorable drug-like characteristics for these compounds.

For potential NMDAR therapeutic agents, Gavestinel, Perzinfotel, and Butylphthalide, were also systematically predicted (Figure 11). The results revealed that all three compounds exhibited favorable ADMET properties. Gavestinel, with its moderate molecular weight, showed a slightly elevated logP value attributed to its hydrophobic groups, leading to marginal water solubility limitations. Despite this, Gavestinel retained its oral bioavailability. Contrarily, Perzinfotel exhibited enhanced water solubility due to the presence of a phosphate group within its molecular structure, which concomitantly resulted in reduced logP and logD values. Lastly, Butylphthalide presented with a logP value on the verge of the upper limit, yet all other properties fell within the scientifically recommended and acceptable range, demonstrating its optimal characteristics.

In conclusion, this comprehensive ADMET analysis offers crucial insights into the pharmacokinetic and safety profiles of these investigational drugs. These findings are instrumental in guiding their further development and optimization for potential use in treating substance addiction.

3 Methods

3.1 DEG analysis and PPI network

The gene expression datasets for our DEG analysis were obtained from the GEO database. For the statistical analysis, we utilized the Limma [77] package to identify DEGs. For opioid addiction, the dataset GSE87823 was used. To minimize potential biases from age and gender, we included only male samples aged between 19 and 25. The gene expression data underwent quantile normalization. The set criteria for significance were a $-\text{Log}_2\text{FoldChange}$ of 2 and a p-value threshold of 0.01. In the analysis of cocaine addiction, we employed the dataset GSE54839 [38]. All samples were incorporated since control subjects were appropriately matched with chronic cocaine abusers. It is noteworthy that quantile normalization had already been applied to this dataset by its provider. The thresholds applied were a $-\text{Log}_2\text{FoldChange}$ of 0.2630344 and a p-value of 0.05. In instances where genes appeared multiple times, we retained only the probe with the highest average expression across samples. Probes associated with multiple genes were excluded. The PPI network among the DEGs was sourced from the STRING database [30]. To facilitate a multi-resolution analysis for each gene set, we employed four distinct interaction confidence thresholds: 0.15, 0.4, 0.7, and 0.9.

3.2 Multiscale topological differentiation of network

The analysis of PPI networks presents significant challenges due to their inherent complexity and the dynamic nature of protein interactions. Their analysis is complicated by factors such as the high-dimensional space they occupy and the variability in interaction strengths. Traditional methods often struggle to capture the nuanced relationships and structural variances within these networks, leading to incomplete or oversimplified interpretations. To overcome these challenges, we propose a multiscale and multi-resolution topological differentiation approach, which leverage the power of PST (or persistent Laplacians) and persistent homology (PH) to analyze the PPI network at various scales, resolutions, and dimensions. By closely examining the difference in topological invariants and geometric features, we can infer the significance of each removed node in a network. Significant alterations in these features typically indicate a high importance of the deleted gene in the network's overall functionality.

3.2.1 Persistent spectral theory

The PPI network is conceptualized as a graph where nodes correspond to proteins, and edges denote the interactions between pairs of proteins. Extending beyond the graph structure, we employ the concept of a simplicial complex to allow high-order interactions in the network, encapsulating a more comprehensive range of shapes and facilitating the inclusion of high-dimensional topological relationships. Persistent spectral theory can capture topological and geometric changes over a continuous range of spatial resolutions, thus revealing the multiscale structure of the data. This is performed by constructing a filtration, which is essentially a nested sequence of simplicial complexes, indexed by a parameter t that typically represents a scale or threshold level. In mathematical terms, a filtration of an oriented simplicial complex K is a collection of sub-complexes $(K_t)_{t \in \mathbb{R}^+}$ satisfying:

$$\emptyset = K_0 \subseteq K_1 \subseteq K_2 \subseteq \dots \subseteq K_m = K. \quad (1)$$

Here, K is the largest simplicial complex achievable from the filtration, with each K_t being a full simplicial complex at the filtration level t .

Accompanying this filtration is a corresponding sequence of chain complexes and boundary operators at each scale t :

$$\dots C_{q+1}^t \xrightleftharpoons[\partial_{q+1}^{t*}]{\partial_{q+1}^t} C_q^t \xrightleftharpoons[\partial_q^{t*}]{\partial_q^t} \dots \xrightleftharpoons[\partial_3^{t*}]{\partial_3^t} C_2^t \xrightleftharpoons[\partial_2^{t*}]{\partial_2^t} C_1^t \xrightleftharpoons[\partial_1^{t*}]{\partial_1^t} C_0^t \xrightleftharpoons[\partial_0^{t*}]{\partial_0^t} \emptyset, \quad (2)$$

where C_q^t denotes the chain group for the sub-complex K_t and ∂_q^t is the q -th boundary operator mapping from C_q^t to C_{q-1}^t . For each K_t , every q -simplex is oriented, and the boundary operator ∂_q^t is applied as follows:

$$\partial_q^t(\sigma_q) = \sum_i^q (-1)^i [v_0, \dots, \hat{v}_i, \dots, v_q], \sigma_q \in K_t.$$

Here, $\sigma_q = [v_0, \dots, v_q]$ is an oriented q -simplex within K_t , and $[v_0, \dots, \hat{v}_i, \dots, v_q]$ represents the oriented $(q-1)$ -simplex obtained by omitting the i -th vertex v_i from σ_q .

Consider \mathbb{C}_q^{t+p} to be the subset of C_q^{t+p} consisting of chains whose boundaries are in C_{q-1}^t :

$$\mathbb{C}_q^{t+p} := \{\alpha \in C_q^{t+p} \mid \partial_q^{t+p}(\alpha) \in C_{q-1}^t\}. \quad (3)$$

The $\bar{\partial}_q^{t+p}$ is defined by:

$$\bar{\partial}_q^{t+p} : \mathbb{C}_q^{t+p} \rightarrow C_{q-1}^t. \quad (4)$$

The p -persistent q -combinatorial Laplacian operator Δ_q^{t+p} along the filtration is given by:

$$\Delta_q^{t+p} = \bar{\partial}_{q+1}^{t+p} (\bar{\partial}_{q+1}^{t+p})^* + \partial_q^{t*} \partial_q^t. \quad (5)$$

The matrix representations of the boundary operators $\bar{\partial}_{q+1}^{t+p}$ and ∂_q^t are \mathcal{B}_{q+1}^{t+p} and \mathcal{B}_q^t , respectively. The p -persistent q -combinatorial Laplacian matrix \mathcal{L}_q^{t+p} is defined as:

$$\mathcal{L}_q^{t+p} = \mathcal{B}_{q+1}^{t+p} (\mathcal{B}_{q+1}^{t+p})^T + (\mathcal{B}_q^t)^T \mathcal{B}_q^t. \quad (6)$$

This matrix is symmetric and positive semi-definite, ensuring that all eigenvalues are real and non-negative. The p -persistent q th Betti numbers, representing the number of q -cycles persisting in K_t after p filtration, correspond to the nullity of \mathcal{L}_q^{t+p} :

$$\beta_q^{t+p} = \dim(\mathcal{L}_q^{t+p}) - \text{rank}(\mathcal{L}_q^{t+p}) = \text{nullity}(\mathcal{L}_q^{t+p}) = \# \text{ of zero eigenvalues of } \mathcal{L}_q^{t+p}. \quad (7)$$

PST provides geometric insights from the spectra of this persistent combinatorial Laplacian, extending beyond mere topological persistence. Persistent Betti numbers offer information on topological constancy, while geometric transformations are discernible through the non-harmonic portions of the spectrum.

3.2.2 Persistent homology

Complementing PST, PH offers a different approach for multiscale analysis through filtration techniques [17]. In this framework, for a given simplicial complex K , we define the q -cycle group \mathcal{Z}_q and the q -boundary group \mathcal{B}_q as the kernel and image of boundary operators ∂_q and ∂_{q+1} , respectively. The equations

$$\mathcal{Z}_q = \text{Ker}\partial_q = \{c \in C_q \mid \partial_q c = 0\}, \quad (8)$$

$$\mathcal{B}_q = \text{Im}\partial_{q+1} = \{c \in C_q \mid \exists d \in C_{q+1} : c = \partial_{q+1} d\}, \quad (9)$$

describe these groups, where C_q represents the set of q -chains. Since $\partial_q \circ \partial_{q+1} = 0$, it follows that $\mathcal{B}_q \subseteq \mathcal{Z}_q \subseteq C_q$. Consequently, we define the q -homology group \mathcal{H}_q as the quotient group:

$$\mathcal{H}_q = \mathcal{Z}_q / \mathcal{B}_q. \quad (10)$$

The q th Betti number β_q is then the rank of \mathcal{H}_q . Furthermore, the persistence of these topological features is quantified by the q th persistence Betti number $\beta_q^{i,j}$, which is the rank of the homology groups of K_i that persist to K_j , formulated as

$$\beta_q^{i,j} = \text{rank}(\mathcal{Z}_q(K_i) / (\mathcal{B}_q(K_j) \cap \mathcal{Z}_q(K_i))). \quad (11)$$

Through filtration, PH provides a detailed perspective on the persistence of topological invariants, though it primarily focuses on the harmonic spectral aspects of PST.

3.2.3 Key gene identification via network topological differentiation

We can make use of PST and/or PH for topological differentiation analysis to assess the significance of individual genes within a PPI network. Using the STRING database, we quantify the interaction strength between protein pairs with a combined score. This score serves as a basis for formulating an abstract distance between proteins, which facilitates the construction of a Rips complex. To conduct a multi-resolution and multiscale analysis, we utilize four PPI network using thresholds of 0.15, 0.4, 0.7, and 0.9. The network can be denoted as $G = (V, E)$. Within this framework, we use a concept known as ‘topological perturbation analysis’, proposed by Chen et al. [78], at the m -th vertex v_m by considering the subgraph G_m that results from eliminating v_m and all edges linked to v_m . For a specified threshold T , we define the distance between two proteins v_i and v_j in G as:

$$D_{ij} = \begin{cases} 1 - s_{ij}, & \text{if } s_{ij} > T. \\ \infty, & \text{otherwise.} \end{cases} \quad (12)$$

where s_{ij} denote the combined score of interaction between proteins v_i and v_j in STRING database. In this study, PST is utilized to derive both topological and geometric characteristics of the network in its original and perturbed states. For the analysis, a Rips complex-based filtration up to two dimensions is established. In each network case, ten filtration parameters are evenly chosen from the interval 0 to $(1 - T)$. From each Laplacian spectrum, we compute the harmonic spectra count and the five statistical descriptors (minimum, maximum, mean, standard deviation, and sum) of the non-harmonic spectra. For every network G , we encapsulate its attributes into a vector f_G , defined as $f_G = \Theta(G)$. Correspondingly, after perturbation at vertex v_m , we obtain the feature vector f_{G_m} for each G_m , defined as $f_{G_m} = \Theta(G_m)$, where Θ encapsulates PST analysis and network vectorization. We quantify the significance of the node v_m by computing the Euclidean distance between feature vectors f_G and f_{G_m} :

$$S_m^G = \text{distance}(f_G, f_{G_m}). \quad (13)$$

This metric reflects the impact of gene v_m within the PPI network G by indicating how its removal alters the network’s structure in terms of topology and geometry.

3.3 Machine learning-based drug repurposing

3.3.1 Data preparation

For our machine learning models, we sourced inhibitor datasets pertaining to mTOR, mGluR5 and NMDAR from the ChEMBL database [79]. These datasets comprise SMILES strings of molecular compounds, each paired with a bioactivity label. The initial labels assigned to these data points were either IC_{50} or K_i values. To adapt these experimental labels into binding affinities (BAs) suitable for our models, we employed the conversion formula: $BA = 1.3633 \times \log_{10} K_i$ (kcal/mol). IC_{50} labels were subsequently estimated to K_i values based on the relationship $K_i = IC_{50}/2$, in alignment with recommendations by Kalliokoski [80]. For instances where a single molecule had multiple bioactivity value labels, we computed the average of these labels. In addition, we retrieved small molecule drugs, categorized under either approved or investigational status, from the DrugBank database (version 5.1.10) [81]. To ensure consistency, their SMILES strings were canonicalized by the RDKit toolkit.

3.3.2 Molecular fingerprints

In our molecular analysis, we employed three fingerprinting methodologies to delineate molecular structures. Two of them harness advanced NLP techniques: one utilizing a bidirectional transformer-based model [82] and the other deploying a sequence-to-sequence autoencoder framework [83]. These NLP-driven methodologies leverage pretrained models to transduce canonical SMILES notations into 512-dimensional latent vectors. Complementing these, our study also incorporated a classical topological approach characterized by the 2D ECFP [84], synthesized via the comprehensive RDKit computational toolkit.

3.3.2.1 Bidirectional transformer Chen and colleagues innovatively crafted a self-supervised learning (SSL) framework for the purpose of pretraining deep neural networks using millions of unlabeled molecular structures [82]. This methodology yields latent vectors derived from input SMILES, encapsulating essential molecular structural details, thereby serving as robust fingerprints for subsequent machine learning applications. The core of their SSL platform employs the bidirectional encoder transformer (BET) model, which leverages attention mechanisms for enhanced accuracy. During the pretraining phase on the SSL platform, the process involved the formation of data pairs comprising authentic SMILES strings and their masked counterparts, with a specific fraction of symbols intentionally obscured. To create these pairs, 15% of the symbols in all SMILES strings were masked. In this masking process, 80% of the symbols were fully obscured, 10% were left unaltered, and the remaining 10% were randomly modified. The employment of the attention mechanism in the BET model ensures that the significance of each symbol within the SMILES string is fully captured. In their study, Chen et al. utilized SMILES strings extracted from one or a combination of the ChEMBL [79], PubChem [85], and ZINC [86] databases for training their SSL-based BET model. In the context of the current study, we opted to utilize the fingerprints generated directly from the pretrained model on ChEMBL database, without any additional fine-tuning (termed as TF-FPs).

3.3.2.2 Sequence-to-sequence auto-encoder A novel unsupervised learning approach, utilizing a sequence-to-sequence autoencoder, has been developed to interpret molecular information encapsulated within the SMILES representation [83]. By translating one molecular format into another, the model efficiently compresses detailed chemical structures into a latent space positioned between the encoder and decoder components. During this transformation, intermediary vectors embed significant physicochemical details, enabling the pretrained model to retrieve molecular descriptors from input SMILES strings without additional training. The encoder employs a combination of convolutional neural network (CNN) and recurrent neural network (RNN) structures, directing their outputs to form intermediary vector representations. On the other hand, the decoder, which is mainly based on RNN architectures, interprets these vectors to produce the desired output. To enhance the richness of the latent vectors, an auxiliary classification module is incor-

porated, forecasting specific molecular properties. The loss function, instrumental during the autoencoder model’s training, is a fusion of cross-entropies associated with the decoder’s probabilistic character outputs and mean squared errors pertinent to molecular property predictions. This comprehensive model has been rigorously trained on expansive datasets sourced from the ZINC and PubChem databases.

3.3.2.3 Extended-connectivity fingerprints Extended-connectivity fingerprints (ECFPs) are a unique class of topological fingerprints used for molecular characterization, primarily developed for structure-activity modeling [84]. The ECFP approach assigns specific identifiers to each atom in a molecule based on their properties and surrounding atoms. Through iterative hashing techniques, these identifiers are updated to encompass the molecule’s neighborhood information, and redundant features are removed. Ultimately, these identifiers are consolidated into a bit array, capturing the molecule’s distinctive features. We employed the RDKit library to produce ECFPs. This library constructs circular fingerprints using the Morgan algorithm, which necessitates a radius parameter dictating the algorithm’s iteration count. In our study, the ECFP radius was set to 2, with the fingerprint length designated at 2048.

3.3.3 Machine learning models

We adopted the GBDT algorithm for constructing our machine learning models [87, 88]. GBDT can be utilized for both regression and classification tasks. The algorithm operates by initially utilizing a weak learner, predominantly a decision tree, to offer primary predictions, subsequently quantifying the residual errors between these initial predictions and the actual outcomes. A subsequent decision tree is tailored to model these residuals, with the explicit objective of correcting inaccuracies introduced by the preceding trees in the sequence. This iterative methodology continues, with each iteration aiming to refine the residuals from the preceding step, until the total tree count attains a predetermined number or the cumulative residuals satisfy a specified threshold. The final model is an aggregate of all the individual trees, which are used for inference on new datasets.

In our investigation, we utilized three molecular fingerprint modalities, namely TF-FP, AE-FP, and ECFP, to represent inhibitor molecules. Three distinct machine learning models were subsequently curated using the GBDT framework. To augment the predictive accuracy and robustness of the models in assessing BAs for mTOR, mGluR5 and NMDAR, a consensus-based approach was adopted. This consensus model combined the predictions by averaging the binding affinity predictions sourced from each of the three individual models.

4 Conclusion

The escalating crisis of drug addiction in the United States calls for effective therapeutic interventions. This study embarked on an comprehensive and rigorous strategy, moving from transcriptomic data analysis to drug discovery, with the goal of identifying potential repurposed drug candidates for opioid and cocaine addiction. The aim is to mitigate the severe societal and health detriments associated with these addictions.

Our sophisticated framework commenced with DEG (Differentially Expressed Gene) analysis on transcriptomic data. We propose a groundbreaking topological differentiation to identify key genes in a multiscale and highly reliable manner. The resulting targets are cross-validated through pathway analysis and literature review. These methodological advancements facilitated the identification of potential new targets, leading to the construction of a comprehensive machine learning repurposing study. We screen potential drugs using Transformer and autoencoder embeddings, along with traditional 2D fingerprints. This marks a pivotal transition from transcriptomic insights to actionable drug repurposing avenues. The resulting promising drug candidates are further screened for their absorption, distribution, metabolism, excretion,

and toxicity (ADMET) properties. This critical evaluation of the pharmacokinetic and safety profiles of identified drug candidates underpins their therapeutic potential.

Through rigorous validation and analysis, three molecular targets, namely mTOR, mGluR5, and NMDAR, were identified as highly relevant to substance addiction. The machine learning models exhibited robust predictive capabilities in evaluating binding affinities, leading to the identification of promising drugs with satisfactory binding energies and favorable pharmacokinetic properties from DrugBank. However, the identified promising drugs need further in vivo validation to ascertain their safety and efficacy in mitigating substance addiction.

Our study signifies an advancement in employing computational methodologies, including advanced topological data analysis, to traverse the continuum from transcriptomic data to drug discovery. It lays down a robust framework for ensuing research aimed at unveiling potent therapeutic interventions, thus underscoring the vital role of interdisciplinary research in navigating the intricate landscape of drug addiction and advancing the drug discovery paradigm. The translational potential of our approach is vast, providing a scalable and adaptable framework that can be applied across a spectrum of diseases and transcriptomic datasets. The transcriptomic data utilized in this study originates from microarray analysis. However, the analytical methodology delineated herein can also be further applied to single-cell RNA sequencing (scRNA-Seq) data, thereby accounting for cellular heterogeneity within tissues. This acknowledgment of cellular heterogeneity is of paramount importance, particularly in the context of neurological diseases, where cell-specific variations significantly impact disease manifestation and progression. In conclusion, our study not only advances the field of addiction therapy but also sets a new benchmark for interdisciplinary research in drug discovery, demonstrating the potential to transform healthcare research paradigms.

5 Data Availability

The data and source code of this study are freely available at GitHub (<https://github.com/Brian-hongyan/DEG-substance-addiction>).

6 Acknowledgements

The work Wei was supported in part by NIH grants R01GM126189, R01AI164266, and R35GM148196, National Science Foundation grants DMS2052983 and IIS-1900473, Michigan State University Research Foundation, and Bristol-Myers Squibb 65109.

7 Conflicts of Interests

The authors declare no competing interests.

Appendix A Literature validation

A.1 Opioid addiction-related key genes

To gain deeper insights into the intricate relationship between our identified key genes and opioid addiction, we turned to literature validation.

One of the intriguing genes that surfaced was RHEB, whose association with opioid addiction appears to be mediated through the mTORC1 pathway. RHEB, a small GTPase, is instrumental in activating mTORC1 [89]. While RHEB's binding to mTOR occurs distally from the kinase's active site, it induces a pronounced global conformational shift [90]. This allosteric modulation realigns active-site residues, enhancing catalytic actions. The significance of this interaction is underscored by the observed linkage between mTORC1 activation and opioid-induced phenomena such as tolerance and hyperalgesia. Diving deeper into the mechanisms, opioids have been postulated to induce alterations in protein translation within the nervous system [91]. These changes are believed to set the stage for the emergence of tolerance and hyperalgesia. Xu et al. unearthed that after repeated morphine administrations, mTOR—a regulator of protein translation—becomes activated in rat spinal dorsal horn neurons [91]. Notably, this mTOR activation is initiated through the μ opioid receptor and is channeled via the intracellular PI3K/Akt pathway. This discovery presents mTOR inhibitors as potential therapeutic agents in stymieing or diminishing opioid tolerance, particularly when addressing chronic pain. Furthermore, the overarching role of mTORC1 extends beyond opioids. Other substances, including cocaine [92, 93], cannabinoids [94], and alcohol [95–97], have also been shown to activate mTORC1. This broad-spectrum influence underscores the pivotal role mTORC1 assumes in the realm of substance addiction.

ADCY9 is an integral protein implicated in the morphine addiction pathway, playing a pivotal role in the cellular signaling cascade. Its primary function is to catalyze the conversion of ATP into cyclic AMP (cAMP) [98]. One of the most noteworthy roles of cAMP is its ability to activate protein kinase A (PKA). When cAMP binds to the regulatory subunits of PKA, it triggers a conformational change, releasing the catalytic subunits. Upon release, these catalytic subunits are rendered active and embark on phosphorylating a myriad of protein targets inside the cell, initiating or modulating various cellular processes. A noteworthy aspect of PKA's function lies in its capability to modulate the dynamics of gamma-aminobutyric acid (GABA) [99–102]. PKA not only influences the secretion of GABA by neuronal cells [100, 101] but also plays a role in fine-tuning the functional responsiveness of GABA receptors [99, 102]. GABA stands out as the principal inhibitory neurotransmitter within the central nervous system [103, 104]. It is instrumental in modulating neuronal excitability, thus maintaining a delicate balance between excitatory and inhibitory signals in the brain. A malfunction or dysregulation in ADCY9's activity could unleash a cascade of molecular events that may disturb this delicate balance. Such an aberration could potentially compromise GABAergic signaling, culminating in a state of hyperexcitability within the central nervous system. This heightened excitability is often accompanied by a surge in the release of dopamine, the neurotransmitter associated with pleasure and reward [105, 106].

The adenomatous polyposis coli (APC) protein is intrinsically tied to opioid addiction through its interactions within the Wnt signaling pathway. Research has highlighted the Wnt pathway's involvement in withdrawal symptoms ensuing from opioid receptor activation, either due to exposure to morphine or as a result of chronic inflammation [107]. Moreover, the manifestation of opioid-induced hyperalgesia, a paradoxical increase in pain sensitivity, has been tied to the activities of reactive astrocytes, which are intriguingly governed by Wnt5a signaling [108]. APC plays a pivotal role in this milieu by acting as a negative regulator of the Wnt pathway. It is a key constituent of the destruction complex, a molecular assembly that also includes the proteins AXIN and Glycogen Synthase Kinase 3β (GSK- 3β) [109, 110]. Within the destruction complex, GSK- 3β phosphorylates specific serine and threonine residues on β -catenin which marks β -catenin for ubiquitination and subsequent degradation.

TBL1XR1 is implicated in opioid addiction through its potential involvement in the Wnt signaling pathway. Some mutations can amplify the activation of the Wnt pathway mediated by TBL1XR1 [111]. While there are indications of its role, a deeper exploration is essential to fully demonstrate TBL1XR1's significance in the context of opioid addiction.

A.2 Cocaine addiction-related key genes

To unravel the intricate interplay between our pinpointed key genes and cocaine addiction, we conducted a detailed literature validation for a comprehensive understanding.

The immediate early gene FOS (c-Fos) has been a significant player in the context of cocaine addiction, as underscored by numerous studies exploring its intricate involvement in cocaine-induced neuroplasticity and behavioral responses [112–116]. Zhang et al. investigated the influence of repeated cocaine administration on the expression of various molecular markers, particularly in Fos-deficient brain environments [113]. The result showed that Fos's absence in the brain results in altered expression levels of several transcription factors, neurotransmitter receptors, and intracellular signaling molecules—all of which are induced by repeated cocaine exposure. This observation suggests that Fos is instrumental in acquiring cocaine-induced persistent changes. Xu demonstrated that the dendritic reorganization of medium spiny neurons, a hallmark of cocaine-induced neuroadaptations, was notably attenuated in Fos-mutant brains [116]. These structural changes, or the lack thereof, were not merely restricted to the molecular domain; they manifested behaviorally as well. Mice with mutant FOS genes exhibited a marked reduction in behavioral sensitization, a phenomenon characterized by an escalating response to repeated cocaine administration.

Interleukin-6 (IL-6) has been suggested to have some connections with cocaine-induced behaviors. Mai et al.'s study on IL-6 knockout mice indicated a potential protective effect against cocaine-induced reactions, hinting at a role of the JAK2/STAT3 and PACAP signaling pathways [117]. Additionally, observed changes in serum levels of IL-6 among cocaine users hint at a peripheral response to the drug [118]. However, the overall evidence linking IL-6 to cocaine effects is still limited, and more research is needed to establish a direct relationship.

Research suggests that SYT1 may influence cognitive performance from cocaine addiction. Silva et al. investigated the link between SYT1-rs2251214 and susceptibility as well as severity (as gauged by the addiction severity index) of CUD in a study involving 315 smoked cocaine addicts and 769 non-addicts [119]. Their findings highlighted a significant association between SYT1-rs2251214 and CUD vulnerability. Additionally, Viola et al. identified a correlation between cognitive performance and SYT1-rs2251214 in women diagnosed with cocaine use disorder [120].

Research has increasingly highlighted the significant role of α -synuclein (SNCA) in various forms of substance addiction, extending beyond cocaine. SNCA is known for its critical involvement in dopaminergic transmission, a pathway often implicated in addictive behaviors [121]. Qin et al. observed that chronic cocaine abuse leads to an upregulation of SNCA expression in the human striatum [122]. This was evidenced by immunoblot analysis in the ventral putamen, revealing elevated SNCA protein levels in striatal synaptosomes of cocaine users compared to age-matched drug-free controls. Additionally, a study by Foroud et al. suggests a link between SNCA variations and alcohol craving [123]. Although alcohol craving is a common feature of alcohol dependence, it is not universally present. Their findings indicate that genetic variation in SNCA could contribute to these craving behaviors, underscoring the gene's broader relevance in substance addiction.

A.3 Integrated Analysis of Opioid and Cocaine Addiction

Extensive literature validation underscores a significant association between GABRB3, PTPRN2, and GLS genes with drug addiction. The GABRB3 gene encodes the β 3 subunit of the GABAA receptor. Chen et

al. highlighted the potential of GABRB3 in heroin dependence, suggesting that its elevated expression may play a pivotal role in the disorder’s pathogenesis [124]. Furthermore, several studies have emphasized the role of GABRB3 in alcoholism. Noble et al. demonstrated that both DRD2 and GABRB3 variants heightened the risk for alcoholism [125]. Similarly, findings by Song et al. linked paternal transmission of GABRB3 to alcoholism [126], while Young and colleagues associated both DRD2 and GABRB3 with alcohol-related expectations [127]. PTPRN2 has emerged as a significant gene in substance dependence and cognitive behavior [128]. Linkage analyses have identified its significance in the comorbidity of cocaine dependence and major depressive episodes in humans [129]. Further, genome-wide association studies have linked PTPRN2 to cognitive performance, risk-taking behaviors, and smoking initiation [130]. Complementing the human findings, studies on PTPRN2 knockout mice have reported reduced concentrations of crucial neurotransmitters such as dopamine, norepinephrine, and serotonin in the brain [131]. Glutaminase (GLS) is an enzyme responsible for the conversion of the amino acid glutamine into glutamate [132]. As the predominant excitatory neurotransmitter in the central nervous system, glutamate plays pivotal roles in the behavioral effects elicited by psychostimulant drugs [133]. Over the past two decades, a combination of fundamental neuroscience research and preclinical studies using animal models has underscored the centrality of glutamate transmission in drug reward mechanisms, reinforcement, and the propensity for relapse [134]. Given that glutaminases are the primary producers of glutamate in the brain, their potential significance in the realm of drug addiction becomes apparent [133]. Glutamate’s effects are mediated through two primary receptor types: ionotropic and metabotropic [135]. The former are ion channels that facilitate ion movement upon glutamate activation, whereas the latter, being G-protein coupled receptors, trigger intricate signal transduction pathways when bound to glutamate. Notably, among these, NMDAR (an ionotropic receptor) and mGluR5 (a metabotropic receptor) are crucial in modulating neuronal excitability. Multiple studies have illuminated their intimate association with substance addiction [44–47, 136–138]. As for IL1B, acute cocaine exposure has been linked to increased IL1B levels in specific brain regions, as shown by Cearley et al.’s findings in the cortex and nucleus accumbens [139]. Montesinos et al. further observed that cocaine-induced changes in CX3CL1 concentrations are related to IL1B levels, suggesting activation of shared inflammatory pathways in the hippocampus [140]. The significance of IL-1B in addiction is further underscored by the findings of Liang et al., who explored its genetic aspects in relation to alcohol dependence [141]. Their study revealed that polymorphisms in IL-1B are associated with a modified risk profile for alcohol dependence. Intriguingly, the particular single nucleotide polymorphisms (SNPs) at positions -511 and -31 are found with greater frequency in opioid-dependent populations. Although the association is described as weak, it nonetheless suggests a potential genetic predisposition linked to an increased risk of opioid dependence. This aligns with our identification of IL1B as a key gene in addiction, revealing its cross-substance implications and reinforcing its potential role as a biomarker or therapeutic target.

Appendix B Topological objects

B.1 Simplicial complex and chain complex

The PPI network is conceptualized as a graph where nodes correspond to proteins, and edges denote the interactions between pairs of proteins. Extending beyond the graph structure, we employ the concept of a simplicial complex to allow high-order interactions in the network, encapsulating a more comprehensive range of shapes and facilitating the inclusion of high-dimensional topological relationships. A simplicial complex is an aggregate of simplices, which are the fundamental building blocks that span various dimensions. Specifically, a q -simplex (denoted as σ_q) can be defined as the convex combination of $(q + 1)$ vertices $(v_0, v_1, v_2, \dots, v_q)$ that are affinely independent, expressed as:

$$\sigma_q := [v_0, v_1, \dots, v_q]. \quad (14)$$

In the realm of Euclidean geometry, simplices correspond to familiar shapes: a 0-simplex represents a point, a 1-simplex forms a line segment, a 2-simplex constitutes a triangle, and a 3-simplex is akin to a tetrahedron. For any given set of $(q + 1)$ points, every non-empty subset can be the vertices of a subsimplex, considered to be a face of a q -simplex, denoted as $\sigma^m \subset \sigma_q$. The structure known as a simplicial complex, denoted by K , is defined as a finite set of simplices that adhere to two critical conditions:

- 1) Any face of a simplex within K must also be included in K ;
- 2) The nonempty intersection of any two simplices is a face of both simplices.

The relationship between simplices within a complex can be characterized by their adjacency, a concept extended from the combinatorial graph theory. In a graph, the degree of a vertex, denoted as $\deg(v)$, is the tally of its adjacent edges. This principle becomes more complex when applied to q -simplices, which are adjacent to both $(q - 1)$ -simplices and $(q + 1)$ -simplices. To navigate this complexity, it is necessary to distinguish between upper and lower adjacencies for defining the degree of a q -simplex when $q > 0$. Two q -simplices, σ_q^1 and σ_q^2 , within a complex K are considered upper adjacent $\sigma_q^1 \overset{U}{\sim} \sigma_q^2$ if they both constitute faces of the same $(q + 1)$ -simplex. Conversely, they are lower adjacent $\sigma_q^1 \overset{L}{\sim} \sigma_q^2$ if they share a common $(q - 1)$ -simplex. The upper degree, $\deg_U(\sigma_q)$, is the count of $(q + 1)$ -simplices of which the q -simplex is a face, while the lower degree, $\deg_L(\sigma_q)$, is the count of its $(q - 1)$ -simplex faces, which invariably equals $(q + 1)$. Consequently, for q -simplices where $q > 0$, the degree is the sum of the upper and lower degrees:

$$\deg(\sigma_q) = \deg_L(\sigma_q) + \deg_U(\sigma_q). \quad (15)$$

The concept of orientation in a simplex is pivotal and is dictated by the sequence of its vertices, excluding the 0-simplex which has no orientation. For a q -simplex σ_q , two given vertex orderings are considered to be similarly oriented if they can be interchanged by an even permutation, hence both configurations represent an orientation of σ_q . If an odd permutation is required, the orderings are dissimilarly oriented. Consequently, an oriented q -simplex is the pairing of a simplex σ_q with a designated orientation. When every simplex within a simplicial complex K is assigned an orientation, we refer to K as an oriented simplicial complex.

In topological, geometric, and algebraic studies, the framework of chain complexes is essential. Consider a simplicial complex K with a maximum dimension of q . Within this context, a q -chain is constructed as a formal summation of the q -simplices in K , utilizing coefficients drawn from the \mathbb{Z}_2 field. The collection of all q -chains, under the addition defined by \mathbb{Z}_2 , forms a group known as the chain group, symbolized by $C_q(K)$. To create connections between chain groups across various dimensions, the boundary operator for q -chains, denoted ∂_q , serves as a mapping function from $C_q(K)$ to $C_{q-1}(K)$. This operator transforms a q -chain, represented as a linear combination of q -simplices, into the corresponding combination of their $(q - 1)$ -dimensional boundaries. For a q -simplex spanned by vertices $[v_0, v_1, \dots, v_q]$, symbolized as σ_q , the action of ∂_q is mathematically articulated as:

$$\partial_q \sigma_q = \sum_{i=0}^q (-1)^i [v_0, \dots, \hat{v}_i, \dots, v_q], \quad (16)$$

where \hat{v}_i indicates the $(q - 1)$ -simplex formed by excluding the vertex v_i from σ_q . A q -chain that yields a zero boundary upon the application of ∂_q is termed a q -cycle.

The structure of a chain complex is characterized by a sequence of chain groups linked by boundary operators. This sequence forms a continuous cascade from higher-dimensional chains down to zero-dimensional chains, which is mathematically depicted as:

$$\dots \xrightarrow{\partial_{q+2}} C_{q+1}(K) \xrightarrow{\partial_{q+1}} C_q(K) \xrightarrow{\partial_q} C_{q-1}(K) \xrightarrow{\partial_{q-1}} \dots \quad (17)$$

In this expression, $C_q(K)$ represents the chain group composed of q -chains in the simplicial complex K , while ∂_q denotes the boundary operator mapping q -chains to $(q - 1)$ -chains. The chain complex terminates with the null set, indicating that the boundary of a 0-chain is inherently zero since there are no negative-dimensional chains. Each boundary operator connects adjacent levels of the complex, ensuring that the boundary of a boundary within this sequence is always zero, a foundational concept in homology theory.

B.2 q -combinatorial Laplacian

In the field of algebraic topology, the boundary operators within a simplicial complex K facilitate the construction of a bridge between different dimensions of chains. The matrix representation of the q -boundary operator $\partial_q : C_q(K) \rightarrow C_{q-1}(K)$ is denoted as \mathcal{B}_q . The dimensions of this matrix—rows corresponding to the number of $(q - 1)$ -simplices and columns to the number of q -simplices—reflect the structure of K . The adjoint of ∂_q , symbolized as $\partial_q^* : C_{q-1}(K) \rightarrow C_q(K)$, operates in the reverse direction of the boundary operator, and its matrix representation is the transpose of \mathcal{B}_q , labeled \mathcal{B}_q^T . Diving deeper into topological invariants, the q -combinatorial Laplacian is a linear transformation $\Delta_q : C_q(K) \rightarrow C_q(K)$ defined as:

$$\Delta_q := \partial_{q+1}\partial_{q+1}^* + \partial_q^*\partial_q. \quad (18)$$

Its matrix form, \mathcal{L}_q , emerges as a summation of the product of boundary matrices and their transposes:

$$\mathcal{L}_q = \mathcal{B}_{q+1}\mathcal{B}_{q+1}^T + \mathcal{B}_q^T\mathcal{B}_q. \quad (19)$$

Specifically, for $q = 0$, the combinatorial Laplacian, also known as the graph Laplacian, simplifies due to ∂_0 being a zero map, resulting in:

$$\mathcal{L}_0 = \mathcal{B}_1\mathcal{B}_1^T. \quad (20)$$

The matrix elements of \mathcal{L}_q are defined by the relationships between simplices and their degrees of connectivity:

$$(\mathcal{L}_q)_{ij} = \begin{cases} \deg(\sigma_q^i) + q + 1, & \text{if } i = j. \\ 1, & \text{if } i \neq j, \sigma_q^i \stackrel{U}{\sim} \sigma_q^j \text{ and } \sigma_q^i \stackrel{L}{\sim} \sigma_q^j \text{ with similar orientation.} \\ -1, & \text{if } i \neq j, \sigma_q^i \stackrel{U}{\sim} \sigma_q^j \text{ and } \sigma_q^i \stackrel{L}{\sim} \sigma_q^j \text{ with dissimilar orientation.} \\ 0, & \text{if } i \neq j \text{ and either } \sigma_q^i \stackrel{U}{\not\sim} \sigma_q^j \text{ or } \sigma_q^i \stackrel{L}{\not\sim} \sigma_q^j. \end{cases} \quad (21)$$

For the graph Laplacian, when $q = 0$, the matrix \mathcal{L}_0 is simplified as:

$$(\mathcal{L}_0)_{ij} = \begin{cases} \deg(\sigma_0^i), & \text{if } i = j. \\ -1, & \text{if } \sigma_0^i \stackrel{U}{\sim} \sigma_0^j. \\ 0, & \text{otherwise.} \end{cases} \quad (22)$$

The q -combinatorial Laplacian matrix is a pivotal element in understanding the intrinsic topological features of a simplicial complex. Due to its symmetric and positive semi-definite nature, it is guaranteed that all eigenvalues of the matrix are real and non-negative. These spectral properties play a central role in revealing the topological invariants of the underlying space. According to the combinatorial Hodge theorem, the Betti numbers, which serve as topological invariants representing the number of q -dimensional holes in a space, can be computed from the spectrum of the Laplacian. The multiplicity of the zero eigenvalue, also known as the nullity of the Laplacian matrix \mathcal{L}_q , corresponds to the q -th Betti number β_q :

$$\beta_q = \dim(\mathcal{L}_q(K)) - \text{rank}(\mathcal{L}_q(K)) = \text{nullity}(\mathcal{L}_q(K)) = \# \text{ of zero eigenvalues of } \mathcal{L}_q(K). \quad (23)$$

These Betti numbers encapsulate crucial topological information. β_0 indicates the number of connected components within the complex. β_1 represents the number of one-dimensional or “circular” holes, often conceptualized as tunnels or loops. β_2 corresponds to the number of two-dimensional voids or “cavities”, akin to the hollow spaces enclosed by surfaces.

Appendix C Datasets for machine learning

In our study, we developed predictive models for binding affinity using inhibitor datasets sourced from the ChEMBL database (Table 7). These models were then applied to estimate the binding affinity of various drugs listed in DrugBank towards three specific targets. The compounds within these datasets were represented using SMILES strings, and their corresponding binding affinities, measured in kcal/mol, were used as the target labels for model training. The distribution of these binding affinity labels across each dataset is depicted in Figure 12.

Table 7: The summary of datasets used in this study.

Dataset	Protein name	Dataset size	Binding affinity range (kcal/mol)
mTOR	Mammalian target of rapamycin	4392	[-5.86, -14.25]
mGluR5	The metabotropic glutamate receptor subtype 5	1777	[-5.47, -13.23]
NMDAR	N-methyl-D-aspartate receptor	2342	[-5.45, -13.32]

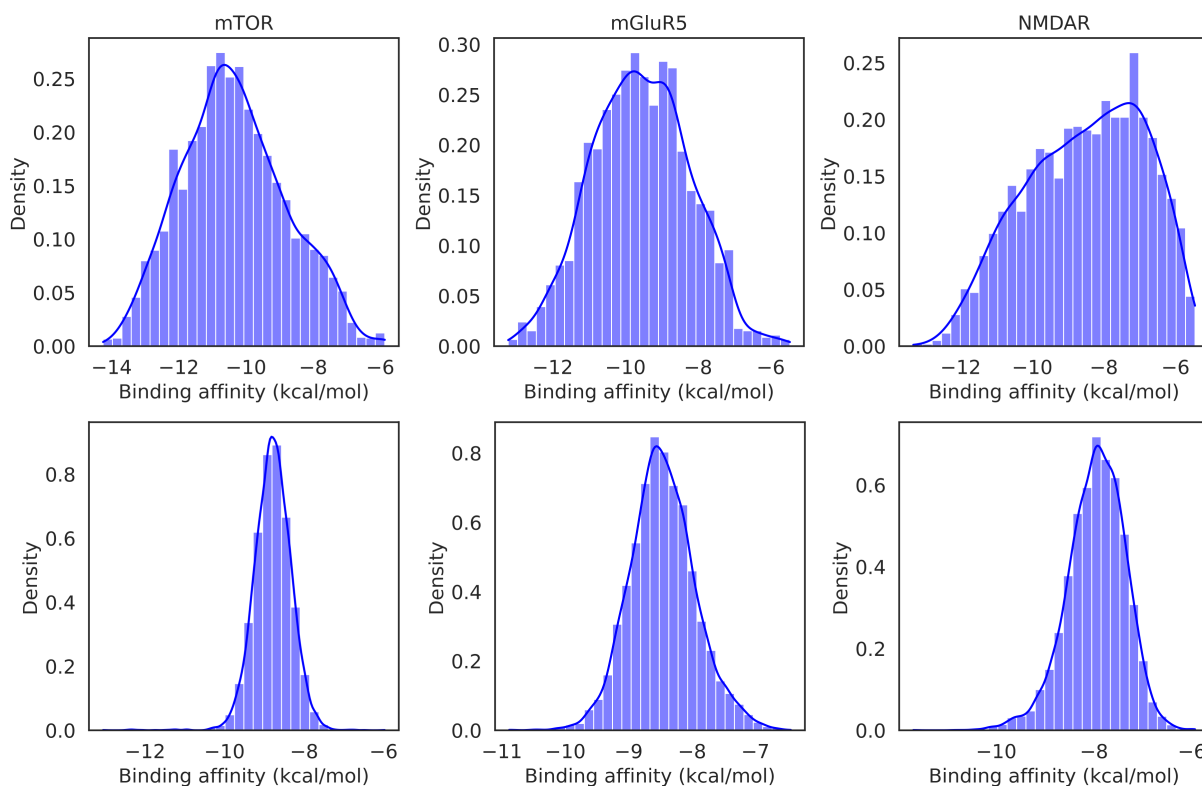


Figure 12: Binding Affinity Distributions in Datasets: The top panel displays the distribution of binding affinity values extracted from the ChEMBL dataset. The bottom panel illustrates the distribution of predicted binding affinities for drugs in DrugBank.

We constructed predictive models for binding affinity using inhibitor datasets obtained from the ChEMBL database. We then utilize these models to predict the binding affinity of drugs in DrugBank to these three targets. The compounds in these datasets are represented by SMILES strings, and their binding affinities (kcal/mol) serve as labels. The distribution of labels for each dataset is illustrated in Figure S1.

Appendix D Evaluation metrics

To assess the performance of our regression models, we employed two key metrics: the Pearson Correlation Coefficient (PCC) and the Root Mean Squared Error (RMSE). The definitions and formulas for these metrics are as follows: The Pearson Correlation Coefficient is defined for two vectors $x = (x_1, x_2, \dots, x_n)$ and $y = (y_1, y_2, \dots, y_n)$ as:

$$R = \text{PCC}(x, y) = \frac{\sum (x_i - \bar{x})(y_i - \bar{y})}{\sqrt{\sum (x_i - \bar{x})^2 \sum (y_i - \bar{y})^2}} \quad (24)$$

where \bar{x} and \bar{y} represent the mean of vectors x and y , respectively. The Root Mean Squared Error (RMSE) is calculated as:

$$\text{RMSE} = \sqrt{\frac{1}{n} \sum_{i=1}^n (y_i - \hat{y}_i)^2}, \quad (25)$$

where y_i is the true value and \hat{y}_i is the predicted value for the i -th sample.

Appendix E Gene significance ranking

We employed topological differentiation to assess the significance of each gene within the PPI network through a multiscale analysis approach. Utilizing networks set at four different thresholds allowed us to conduct a comprehensive multi-resolution analysis. The key genes were identified by intersecting the top 25 genes from each of these four threshold-defined networks, ensuring a robust and consistent selection of significant genes (Table 8, 9).

Table 8: Top 25 Key Genes in the Opioid Addiction-Related DEG PPI Network. The key genes were identified as the intersection of the top-ranking genes across four networks, each defined by different threshold levels.

Ranking	Threshold 0.15	Threshold 0.4	Threshold 0.7	Threshold 0.9
1	YWHAZ	PML	BUB1	PML
2	MAP2K1	YWHAZ	PML	STAT6
3	NTRK2	EIF5B	EIF5B	BUB1
4	PGK1	PECAM1	STAT6	EIF5B
5	UBE2N	BUB1	NCOA1	NCOA1
6	BUB1	ADCY9	RHEB	LRP6
7	TPM2	NTRK2	SRD5A1	TP63
8	TP63	TBL1XR1	APC	RHEB
9	IL4	MCM5	ADCY9	SRD5A1
10	PPP3CA	NCOA1	MCM5	SORT1
11	MYH11	RPL35A	YWHAZ	WNT8B
12	REL	MKI67	TBL1XR1	ARNT
13	SOX5	IL4	PRKAR1A	CDKN1C
14	PECAM1	SIL1	TCAP	HSD17B6
15	PIDD1	RAPGEF3	NPAS2	ADCY9
16	APC	APC	TP63	APC
17	WDFY3	DOHH	DDX28	TBL1XR1
18	HMGB1	HBEGF	SORT1	NPAS2
19	TBL1XR1	STAT6	CDKN1C	RBM25
20	RAB40B	NPAS2	HSD17B6	DOHH
21	ADCY9	RHEB	RBM25	EIF5A2
22	MKI67	PRKAR1A	UBE2N	LUC7L3
23	RET	EIF5A2	RET	IL4
24	RHEB	PGK1	ARNT	NTRK2
25	PRDX3	NOC4L	H2AFV	EIF1AX

Table 9: Top 25 Key Genes in the Cocaine Addiction-Related DEG PPI Network. The key genes were identified as the intersection of the top-ranking genes across four networks, each defined by different threshold levels.

Ranking	Threshold 0.15	Threshold 0.4	Threshold 0.7	Threshold 0.9
1	SNAP25	SNAP25	JUN	JUN
2	JUN	JUN	IL6	IL6
3	IL6	IL6	SNAP25	VAMP2
4	GRIN1	BDNF	VAMP2	SYT1
5	FOS	GRIN1	SYT1	FOS
6	YWHAH	SYP	FGF2	CD44
7	BDNF	SNCA	BDNF	FGF2
8	SYT1	IL1B	CD44	SNAP25
9	GAD2	CD44	SNCA	EGR1
10	DNM1	SYN1	FOS	SNCA
11	MAST1	SOX2	EGR1	IRF1
12	SYP	GAP43	CDK5	IL1B
13	SNCA	CALM3	PAK1	CACNG2
14	ENO2	FGF2	SLC32A1	DNM1
15	IL1B	FOS	VCAM1	CDK5
16	STMN2	SYT1	GRIN1	PAK1
17	SNCB	SLC32A1	GAD2	CCL2
18	NTRK2	VAMP2	STXBP1	JUNB
19	SYN1	GAD2	DNM1	SLC6A3
20	GAP43	EDN1	BAG3	BAG3
21	ATP2B2	DNM1	CACNG2	CXCL10
22	GABRG2	STXBP1	CALM3	STXBP1
23	CALM3	KCNQ2	DNAJB1	CDKN1A
24	KCNQ2	TH	SYP	HSPA1A
25	SLC32A1	SNCB	HSPA1A	NCAN

References

- [1] A Thomas McLellan, David C Lewis, Charles P O'brien, and Herbert D Kleber. Drug dependence, a chronic medical illness: implications for treatment, insurance, and outcomes evaluation. *Jama*, 284(13):1689–1695, 2000.
- [2] Paulette A Zaki, Edward J Bilsky, Todd W Vanderah, Josephine Lai, Christopher J Evans, and Frank Porreca. Opioid receptor types and subtypes: the delta receptor as a model. *Annual review of pharmacology and toxicology*, 36(1):379–401, 1996.
- [3] Vania Modesto-Lowe, Donna Brooks, and Nancy Petry. Methadone deaths: risk factors in pain and addicted populations. *Journal of general internal medicine*, 25:305–309, 2010.
- [4] Richard P Mattick, Courtney Breen, Jo Kimber, and Marina Davoli. Buprenorphine maintenance versus placebo or methadone maintenance for opioid dependence. *Cochrane database of systematic reviews*, (2), 2014.
- [5] David R Gastfriend. Intramuscular extended-release naltrexone: current evidence. *Annals of the New York Academy of Sciences*, 1216(1):144–166, 2011.

- [6] Heraclito Barbosa de Carvalho and Sergio Dario Seibel. Crack cocaine use and its relationship with violence and hiv. *Clinics*, 64(9):857–866, 2009.
- [7] Thijs Beuming, Julie Kniazeff, Marianne L Bergmann, Lei Shi, Luis Gracia, Klaudia Raniszewska, Amy Hauck Newman, Jonathan A Javitch, Harel Weinstein, Ulrik Gether, et al. The binding sites for cocaine and dopamine in the dopamine transporter overlap. *Nature neuroscience*, 11(7):780–789, 2008.
- [8] Anders S Kristensen, Jacob Andersen, Trine N Jørgensen, Lena Sørensen, Jacob Eriksen, Claus J Loland, Kristian Strømgaard, and Ulrik Gether. Slc6 neurotransmitter transporters: structure, function, and regulation. *Pharmacological reviews*, 63(3):585–640, 2011.
- [9] J Martin Elliott and Thomas JR Beveridge. Psychostimulants and monoamine transporters: upsetting the balance. *Current opinion in pharmacology*, 5(1):94–100, 2005.
- [10] Mary Hongying Cheng, Ethan Block, Feizhuo Hu, Murat Can Cobanoglu, Alexander Sorkin, and Ivet Bahar. Insights into the modulation of dopamine transporter function by amphetamine, orphenadrine, and cocaine binding. *Frontiers in neurology*, 6:134, 2015.
- [11] David Matuskey, Jean-Dominique Gallezot, Brian Pittman, Wendol Williams, Jane Wanyiri, Edward Gaiser, Dianne E Lee, Jonas Hannestad, Keunpoong Lim, Minq-Qiang Zheng, et al. Dopamine d3 receptor alterations in cocaine-dependent humans imaged with [11c](+) phno. *Drug and alcohol dependence*, 139:100–105, 2014.
- [12] Patricia A Broderick, Omotola Hope, Catherine Okonji, David N Rahni, and Yueping Zhou. Clozapine and cocaine effects on dopamine and serotonin release in nucleus accumbens during psychostimulant behavior and withdrawal. *Progress in Neuro-Psychopharmacology and Biological Psychiatry*, 28(1):157–171, 2004.
- [13] Francesco Leri, Joseph Flores, Demetra Rodaros, and Jane Stewart. Blockade of stress-induced but not cocaine-induced reinstatement by infusion of noradrenergic antagonists into the bed nucleus of the stria terminalis or the central nucleus of the amygdala. *Journal of Neuroscience*, 22(13):5713–5718, 2002.
- [14] Kyle M Kampman, Charles Dackis, Kevin G Lynch, Helen Pettinati, Carlos Tirado, Peter Gariti, Thorne Sparkman, Michal Atzram, and Charles P O’Brien. A double-blind, placebo-controlled trial of amantadine, propranolol, and their combination for the treatment of cocaine dependence in patients with severe cocaine withdrawal symptoms. *Drug and alcohol dependence*, 85(2):129–137, 2006.
- [15] Xiuning Zhang, Hailei Yu, Rui Bai, and Chunling Ma. Identification and characterization of biomarkers and their role in opioid addiction by integrated bioinformatics analysis. *Frontiers in Neuroscience*, 14:608349, 2020.
- [16] Xu Wang, Shibin Sun, Hongwei Chen, Bei Yun, Zihan Zhang, Xiaoxi Wang, Yifan Wu, Junjie Lv, Yuehan He, Wan Li, et al. Identification of key genes and therapeutic drugs for cocaine addiction using integrated bioinformatics analysis. *Frontiers in Neuroscience*, 17, 2023.
- [17] Afra Zomorodian and Gunnar Carlsson. Computing persistent homology. In *Proceedings of the twentieth annual symposium on Computational geometry*, pages 347–356, 2004.
- [18] Rui Wang, Duc Duy Nguyen, and Guo-Wei Wei. Persistent spectral graph. *International journal for numerical methods in biomedical engineering*, 36(9):e3376, 2020.
- [19] Yuchi Qiu and Guo-Wei Wei. Persistent spectral theory-guided protein engineering. *Nature Computational Science*, pages 1–15, 2023.
- [20] Jiahui Chen, Yuchi Qiu, Rui Wang, and Guo-Wei Wei. Persistent laplacian projected omicron ba. 4 and ba. 5 to become new dominating variants. *Computers in Biology and Medicine*, 151:106262, 2022.

- [21] Zhenyu Meng and Kelin Xia. Persistent spectral-based machine learning (perspect ml) for protein-ligand binding affinity prediction. *Science advances*, 7(19):eabc5329, 2021.
- [22] Zailiang Zhu, Bozheng Dou, Yukang Cao, Jian Jiang, Yueying Zhu, Dong Chen, Hongsong Feng, Jie Liu, Bengong Zhang, Tianshou Zhou, et al. Tidal: Topology-inferred drug addiction learning. *Journal of Chemical Information and Modeling*, 63(5):1472–1489, 2023.
- [23] Sean Cottrell, Rui Wang, and Guowei Wei. Plpca: Persistent laplacian enhanced-pca for microarray data analysis. *arXiv preprint arXiv:2306.06292*, 2023.
- [24] Sudeep Pushpakom, Francesco Iorio, Patrick A Eyers, K Jane Escott, Shirley Hopper, Andrew Wells, Andrew Doig, Tim Williams, Joanna Latimer, Christine McNamee, et al. Drug repurposing: progress, challenges and recommendations. *Nature reviews Drug discovery*, 18(1):41–58, 2019.
- [25] Hongsong Feng, Jian Jiang, and Guo-Wei Wei. Machine-learning repurposing of drugbank compounds for opioid use disorder. *Computers in biology and medicine*, 160:106921, 2023.
- [26] Gabrielle D Gibson, E Zayra Millan, and Gavan P McNally. The nucleus accumbens shell in reinstatement and extinction of drug seeking. *European Journal of Neuroscience*, 50(3):2014–2022, 2019.
- [27] Walter Sneader. The discovery of heroin. *The Lancet*, 352(9141):1697–1699, 1998.
- [28] PROF PO WOLFF. Heroin from the international point of view. *British Journal of Addiction to Alcohol & Other Drugs*, 53(1):51–63, 1956.
- [29] Michele Stanislaw Milella, Ginevra D’Ottavio, Silvana De Pirro, Massimo Barra, Daniele Caprioli, and Aldo Badiani. Heroin and its metabolites: relevance to heroin use disorder. *Translational Psychiatry*, 13(1):120, 2023.
- [30] Damian Szklarczyk, Rebecca Kirsch, Mikaela Koutrouli, Katerina Nastou, Farrokh Mehryary, Radja Hachilif, Annika L Gable, Tao Fang, Nadezhda T Doncheva, Sampo Pyysalo, et al. The string database in 2023: protein–protein association networks and functional enrichment analyses for any sequenced genome of interest. *Nucleic acids research*, 51(D1):D638–D646, 2023.
- [31] Hylan C Moises, Konstantin I Rusin, and RL Macdonald. Mu-and kappa-opioid receptors selectively reduce the same transient components of high-threshold calcium current in rat dorsal root ganglion sensory neurons. *Journal of Neuroscience*, 14(10):5903–5916, 1994.
- [32] Gerald W Zamponi and Terrance P Snutch. Modulating modulation: crosstalk between regulatory pathways of presynaptic calcium channels. *Molecular interventions*, 2(8):476, 2002.
- [33] C König, O Gavrilova-Ruch, G Segond Von Banchet, R Bauer, M Grün, E Hirsch, I Rubio, S Schulz, SH Heinemann, HG Schaible, et al. Modulation of μ -opioid receptor desensitization in peripheral sensory neurons by phosphoinositide 3-kinase γ . *Neuroscience*, 169(1):449–454, 2010.
- [34] Sreedhar Madishetti, Nadine Schneble, Christian König, Emilio Hirsch, Stefan Schulz, Jörg P Müller, and Reinhard Wetzker. Pi3k γ integrates c amp and akt signalling of the μ -opioid receptor. *British journal of pharmacology*, 171(13):3328–3337, 2014.
- [35] Mayumi Miyatake, Tal J Rubinstein, Gregory P McLennan, Mariana M Belcheva, and Carmine J Coscia. Inhibition of egf-induced erk/map kinase-mediated astrocyte proliferation by μ opioids: integration of g protein and β -arrestin 2-dependent pathways. *Journal of neurochemistry*, 110(2):662–674, 2009.
- [36] Nahid A Shahabi, Kathy McAllen, and Burt M Sharp. δ opioid receptors stimulate akt-dependent phosphorylation of c-jun in t cells. *Journal of Pharmacology and Experimental Therapeutics*, 316(2):933–939, 2006.

- [37] Miao Tan, Wendy M Walwyn, Christopher J Evans, and Cui-Wei Xie. p38 mapk and β -arrestin 2 mediate functional interactions between endogenous μ -opioid and α 2a-adrenergic receptors in neurons. *Journal of biological chemistry*, 284(10):6270–6281, 2009.
- [38] Michael J Bannon, Magen M Johnson, Sharon K Michelhaugh, Zachary J Hartley, Steven D Halter, James A David, Gregory Kapatos, and Carl J Schmidt. A molecular profile of cocaine abuse includes the differential expression of genes that regulate transcription, chromatin, and dopamine cell phenotype. *Neuropsychopharmacology*, 39(9):2191–2199, 2014.
- [39] Alexey Bingor, Matityahu Azriel, Lavi Amiad, and Rami Yaka. Potentiated response of erk/mapk signaling is associated with prolonged withdrawal from cocaine behavioral sensitization. *Journal of Molecular Neuroscience*, pages 1–8, 2021.
- [40] Wei-Lun Sun, Pamela M Quizon, and Jun Zhu. Molecular mechanism: Erk signaling, drug addiction, and behavioral effects. *Progress in molecular biology and translational science*, 137:1–40, 2016.
- [41] Keren Bachi, Venkatesh Mani, Devi Jeyachandran, Zahi A Fayad, Rita Z Goldstein, and Nelly Alia-Klein. Vascular disease in cocaine addiction. *Atherosclerosis*, 262:154–162, 2017.
- [42] Bryan G Schwartz, Shereif Rezkalla, and Robert A Kloner. Cardiovascular effects of cocaine. *Circulation*, 122(24):2558–2569, 2010.
- [43] Gil M Lewitus, Sarah C Konefal, Andrew D Greenhalgh, Horia Pribiag, Keanan Augereau, and David Stellwagen. Microglial tnf- α suppresses cocaine-induced plasticity and behavioral sensitization. *Neuron*, 90(3):483–491, 2016.
- [44] Claire M Corbett, Emily ND Miller, and Jessica A Loweth. mglu5 inhibition in the basolateral amygdala prevents estrous cycle-dependent changes in cue-induced cocaine seeking. *Addiction neuroscience*, 5:100055, 2023.
- [45] Michael J Glass. Opioid dependence and nmda receptors. *ILAR journal*, 52(3):342–351, 2011.
- [46] Hideaki Kato, Minoru Narita, Kan Miyoshi, Megumi Asato, Nana Hareyama, Hiroyuki Nozaki, Tomoe Takagi, Masami Suzuki, and T Suzuki. Implication of src family kinase-dependent phosphorylation of nr2b subunit-containing nmda receptor in the rewarding effect of morphine. *Nihon shinkei seishin yakurigaku zasshi= Japanese journal of psychopharmacology*, 26(3):119–124, 2006.
- [47] Yoan Mihov and Gregor Hasler. Negative allosteric modulators of metabotropic glutamate receptors subtype 5 in addiction: a therapeutic window. *International Journal of Neuropsychopharmacology*, 19(7):pyw002, 2016.
- [48] Darren R Flower. *Drug design: cutting edge approaches*, volume 279. Royal Society of Chemistry, 2002.
- [49] Jost Klawitter, Björn Nashan, and Uwe Christians. Everolimus and sirolimus in transplantation-related but different. *Expert opinion on drug safety*, 14(7):1055–1070, 2015.
- [50] Jeffrey P MacKeigan and Darcy A Krueger. Differentiating the mtor inhibitors everolimus and sirolimus in the treatment of tuberous sclerosis complex. *Neuro-oncology*, 17(12):1550–1559, 2015.
- [51] Felix A Mensah, Jean-Pierre Blaize, and Locke J Bryan. Spotlight on copanlisib and its potential in the treatment of relapsed/refractory follicular lymphoma: evidence to date. *OncoTargets and therapy*, pages 4817–4827, 2018.
- [52] Matteo Bassetti, Elda Righi, Davide Pecori, and Glenn Tillotson. Delafloxacin: an improved fluoroquinolone developed through advanced molecular engineering. *Future Microbiology*, 13(10):1081–1094, 2018.

- [53] LJ Scott. Delafloxacin: a review in acute bacterial skin and skin structure infections. *Drugs*, 80:1247–1258, 2020.
- [54] Anthony J Lembo, Brian E Lacy, Marc J Zuckerman, Ron Schey, Leonard S Dove, David A Andrae, J Michael Davenport, Gail McIntyre, Rocio Lopez, Lisa Turner, et al. Eluxadoline for irritable bowel syndrome with diarrhea. *New England Journal of Medicine*, 374(3):242–253, 2016.
- [55] Janet E Dancey and Jose Monzon. Ridaforolimus: a promising drug in the treatment of soft-tissue sarcoma and other malignancies. *Future Oncology*, 7(7):827–839, 2011.
- [56] Pamela Munster, Rahul Aggarwal, David Hong, Jan HM Schellens, Ruud Van Der Noll, Jennifer Specht, Petronella O Witteveen, Theresa L Werner, E Claire Dees, Emily Bergsland, et al. First-in-human phase i study of gsk2126458, an oral pan-class i phosphatidylinositol-3-kinase inhibitor, in patients with advanced solid tumor malignancies. *Clinical Cancer Research*, 22(8):1932–1939, 2016.
- [57] Geoffrey I Shapiro, Katherine M Bell-McGuinn, Julian R Molina, Johanna Bendell, James Spicer, Eunice L Kwak, Susan S Pandya, Robert Millham, Gary Borzillo, Kristen J Pierce, et al. First-in-human study of pf-05212384 (pki-587), a small-molecule, intravenous, dual inhibitor of pi3k and mtor in patients with advanced cancer. *Clinical Cancer Research*, 21(8):1888–1895, 2015.
- [58] Zev A Wainberg, Maria Alsina, Heloisa P Soares, Irene Braña, Carolyn D Britten, Gianluca Del Conte, Patrick Ezeh, Brett Houk, Kenneth A Kern, Stephen Leong, et al. A multi-arm phase i study of the pi3k/mtor inhibitors pf-04691502 and gedatolisib (pf-05212384) plus irinotecan or the mek inhibitor pd-0325901 in advanced cancer. *Targeted oncology*, 12:775–785, 2017.
- [59] Aranapakam M Venkatesan, Zecheng Chen, Osvaldo Dos Santos, Christoph Dehnhardt, Efren Delos Santos, Semiramis Ayril-Kaloustian, Robert Mallon, Irwin Hollander, Larry Feldberg, Judy Lucas, et al. Pki-179: an orally efficacious dual phosphatidylinositol-3-kinase (pi3k)/mammalian target of rapamycin (mtor) inhibitor. *Bioorganic & medicinal chemistry letters*, 20(19):5869–5873, 2010.
- [60] Ming-Tain Lai, Meizhen Feng, Jean-Pierre Falgoutyret, Paul Tawa, Marc Witmer, Daniel DiStefano, Yuan Li, Jason Burch, Nancy Sachs, Meiqing Lu, et al. In vitro characterization of mk-1439, a novel hiv-1 nonnucleoside reverse transcriptase inhibitor. *Antimicrobial agents and chemotherapy*, 58(3):1652–1663, 2014.
- [61] Carolina Scala, Umberto Leone Roberti Maggiore, Valentino Remorgida, Pier Luigi Venturini, and Simone Ferrero. Drug safety evaluation of desogestrel. *Expert opinion on drug safety*, 12(3):433–444, 2013.
- [62] Elyse Swallow, Oscar Patterson-Lomba, Lei Yin, Rina Mehta, Corey Pelletier, David Kao, James K Sheffield, Tim Stonehouse, and James Signorovitch. Comparative safety and efficacy of ozanimod versus fingolimod for relapsing multiple sclerosis. *Journal of Comparative Effectiveness Research*, 9(4):275–285, 2020.
- [63] Julia Paik. Ozanimod: a review in ulcerative colitis. *Drugs*, 82(12):1303–1313, 2022.
- [64] Baltazar Gomez-Mancilla, Elizabeth Berry-Kravis, Randi Hagerman, Florian von Raison, George Apostol, Mike Ufer, Fabrizio Gasparini, and Sébastien Jacquemont. Development of mavoglurant and its potential for the treatment of fragile x syndrome. *Expert opinion on investigational drugs*, 23(1):125–134, 2014.
- [65] Ahmed Negida, Hazem S Ghaith, Salma Yousry Fala, Hussien Ahmed, Eshak I Bahbah, Mahmoud Ahmed Ebada, and Mohamed Abd Elalem Aziz. Mavoglurant (afq056) for the treatment of levodopa-induced dyskinesia in patients with parkinson’s disease: a meta-analysis. *Neurological Sciences*, 42(8):3135–3143, 2021.

- [66] François Tison, Charlotte Keywood, Mark Wakefield, Franck Durif, Jean-Christophe Corvol, Karla Eggert, Mark Lew, Stuart Isaacson, Erwan Bezar, Sonia-Maria Poli, et al. A phase 2a trial of the novel mglur5-negative allosteric modulator dipraglurant for levodopa-induced dyskinesia in parkinson's disease. *Movement Disorders*, 31(9):1373–1380, 2016.
- [67] Martin Platten and Gerd Fätkenheuer. Lersivirine—a new drug for hiv infection therapy. *Expert opinion on investigational drugs*, 22(12):1687–1694, 2013.
- [68] JGD Birkmayer, C Vrecko, D Volc, and W Birkmayer. Nicotinamide adenine dinucleotide (nadh)-a new therapeutic approach to parkinson's disease: Comparison of oral and parenteral application. *Acta Neurologica Scandinavica*, 87:32–35, 1993.
- [69] Lesley J Scott and Caroline M Perry. Delavirdine: a review of its use in hiv infection. *Drugs*, 60(6):1411–1444, 2000.
- [70] Sujuan Rao, Zhijuan Cui, Longmiao Zhang, Shuo Ma, Shuangbo Huang, Li Feng, Yiling Chen, Jinxi Luo, Jinfeng Li, Shiyu Qian, et al. Effects of dietary adenosine and adenosine 5'-monophosphate supplementation on carcass characteristics, meat quality, and lipid metabolism in adipose tissues of finishing pigs. *Meat Science*, 201:109174, 2023.
- [71] GM Bressa. S-adenosyl-l-methionine (same) as antidepressant: meta-analysis of clinical studies. *Acta Neurologica Scandinavica*, 89(S154):7–14, 1994.
- [72] Romano Di Fabio, Anna M Capelli, Nadia Conti, Alfredo Cugola, Daniele Donati, Aldo Feriani, Paola Gastaldi, Giovanni Gaviraghi, Cheryl T Hewkin, Fabrizio Micheli, et al. Substituted indole-2-carboxylates as in vivo potent antagonists acting as the strychnine-insensitive glycine binding site. *Journal of medicinal chemistry*, 40(6):841–850, 1997.
- [73] William A Kinney, Magid Abou-Gharbia, Deanna T Garrison, Jean Schmid, Dianne M Kowal, Donna R Bramlett, Tracy L Miller, Rene P Tasse, Margaret M Zaleska, and John A Moyer. Design and synthesis of [2-(8, 9-dioxo-2, 6-diazabicyclo [5.2. 0] non-1 (7)-en-2-yl)-ethyl] phosphonic acid (eaa-090), a potent n-methyl-d-aspartate antagonist, via the use of 3-cyclobutene-1, 2-dione as an achiral α -amino acid bioisostere. *Journal of medicinal chemistry*, 41(2):236–246, 1998.
- [74] Xi-Qian Chen, Ke Qiu, Hui Liu, Qiang He, Jia-Hui Bai, and Wei Lu. Application and prospects of butylphthalide for the treatment of neurologic diseases. *Chinese medical journal*, 132(12):1467–1477, 2019.
- [75] Anxin Wang, Baixue Jia, Xuelei Zhang, Xiaochuan Huo, Jianhuang Chen, Liqiang Gui, Yefeng Cai, Zaiyu Guo, Yuqing Han, Zhaolong Peng, et al. Efficacy and safety of butylphthalide in patients with acute ischemic stroke: A randomized clinical trial. *JAMA neurology*, 2023.
- [76] Guoli Xiong, Zhenxing Wu, Jiakai Yi, Li Fu, Zhijiang Yang, Changyu Hsieh, Mingzhu Yin, Xiangxiang Zeng, Chengkun Wu, Aiping Lu, et al. Admetlab 2.0: an integrated online platform for accurate and comprehensive predictions of admet properties. *Nucleic Acids Research*, 49(W1):W5–W14, 2021.
- [77] Matthew E Ritchie, Belinda Phipson, DI Wu, Yifang Hu, Charity W Law, Wei Shi, and Gordon K Smyth. limma powers differential expression analyses for rna-sequencing and microarray studies. *Nucleic acids research*, 43(7):e47–e47, 2015.
- [78] Dong Chen, Jian Liu, Jie Wu, Guo-Wei Wei, Feng Pan, and Shing-Tung Yau. Path topology in molecular and materials sciences. *The Journal of Physical Chemistry Letters*, 14(4):954–964, 2023.
- [79] David Mendez, Anna Gaulton, A Patrícia Bento, Jon Chambers, Marleen De Veij, Eloy Félix, María Paula Magariños, Juan F Mosquera, Prudence Mutowo, Michał Nowotka, et al. ChEMBL: towards direct deposition of bioassay data. *Nucleic acids research*, 47(D1):D930–D940, 2019.

- [80] Tuomo Kallioikoski, Christian Kramer, Anna Vulpetti, and Peter Gedeck. Comparability of mixed ic50 data—a statistical analysis. *PloS one*, 8(4):e61007, 2013.
- [81] David S Wishart, Yannick D Feunang, An C Guo, Elvis J Lo, Ana Marcu, Jason R Grant, Tanvir Sajed, Daniel Johnson, Carin Li, Zinat Sayeeda, et al. Drugbank 5.0: a major update to the drugbank database for 2018. *Nucleic acids research*, 46(D1):D1074–D1082, 2018.
- [82] Dong Chen, Jiaxin Zheng, Guo-Wei Wei, and Feng Pan. Extracting predictive representations from hundreds of millions of molecules. *The journal of physical chemistry letters*, 12(44):10793–10801, 2021.
- [83] Robin Winter, Floriane Montanari, Frank Noé, and Djork-Arné Clevert. Learning continuous and data-driven molecular descriptors by translating equivalent chemical representations. *Chemical science*, 10(6):1692–1701, 2019.
- [84] David Rogers and Mathew Hahn. Extended-connectivity fingerprints. *Journal of chemical information and modeling*, 50(5):742–754, 2010.
- [85] Sunghwan Kim, Paul A Thiessen, Evan E Bolton, Jie Chen, Gang Fu, Asta Gindulyte, Lianyi Han, Jane He, Siqian He, Benjamin A Shoemaker, et al. Pubchem substance and compound databases. *Nucleic acids research*, 44(D1):D1202–D1213, 2016.
- [86] John J Irwin and Brian K Shoichet. Zinc- a free database of commercially available compounds for virtual screening. *Journal of chemical information and modeling*, 45(1):177–182, 2005.
- [87] Jerome H Friedman. Greedy function approximation: a gradient boosting machine. *Annals of statistics*, pages 1189–1232, 2001.
- [88] Guolin Ke, Qi Meng, Thomas Finley, Taifeng Wang, Wei Chen, Weidong Ma, Qiwei Ye, and Tie-Yan Liu. Lightgbm: A highly efficient gradient boosting decision tree. *Advances in neural information processing systems*, 30, 2017.
- [89] Xiaqing Ma, Wenjie Du, Wenying Wang, Limin Luo, Min Huang, Haiyan Wang, Raozhou Lin, Zhongping Li, Haibo Shi, Tifei Yuan, et al. Persistent rheb-induced mtorc1 activation in spinal cord neurons induces hypersensitivity in neuropathic pain. *Cell death & disease*, 11(9):747, 2020.
- [90] Haijuan Yang, Xiaolu Jiang, Buren Li, Hyo J Yang, Meredith Miller, Angela Yang, Ankita Dhar, and Nikola P Pavletich. Mechanisms of mtorc1 activation by rheb and inhibition by pras40. *Nature*, 552(7685):368–373, 2017.
- [91] Ji-Tian Xu, Jian-Yuan Zhao, Xiuli Zhao, Davinna Ligons, Vinod Tiwari, Fidelis E Atianjoh, Chun-Yi Lee, Lingli Liang, Weidong Zang, Dolores Njoku, et al. Opioid receptor–triggered spinal mtorc1 activation contributes to morphine tolerance and hyperalgesia. *The Journal of clinical investigation*, 124(2):592–603, 2014.
- [92] Jeffrey Bailey, Dzwokai Ma, and Karen K Szumlinski. Rapamycin attenuates the expression of cocaine-induced place preference and behavioral sensitization. *Addiction biology*, 17(2):248–258, 2012.
- [93] Jinfang Wu, Sarah E McCallum, Stanley D Glick, and Yunfei Huang. Inhibition of the mammalian target of rapamycin pathway by rapamycin blocks cocaine-induced locomotor sensitization. *Neuroscience*, 172:104–109, 2011.
- [94] Salman Zubedat and Irit Akirav. The involvement of cannabinoids and mtor in the reconsolidation of an emotional memory in the hippocampal–amygdala–insular circuit. *European neuropsychopharmacology*, 27(4):336–349, 2017.

- [95] Jérémie Neasta, Sami Ben Hamida, Quinn Yowell, Sebastien Carnicella, and Dorit Ron. Role for mammalian target of rapamycin complex 1 signaling in neuroadaptations underlying alcohol-related disorders. *Proceedings of the National Academy of Sciences*, 107(46):20093–20098, 2010.
- [96] Jeremie Neasta, Segev Barak, Sami Ben Hamida, and Dorit Ron. mtor complex 1: a key player in neuroadaptations induced by drugs of abuse. *Journal of neurochemistry*, 130(2):172–184, 2014.
- [97] Rainer Spanagel. Alcoholism: a systems approach from molecular physiology to addictive behavior. *Physiological reviews*, 89(2):649–705, 2009.
- [98] Beth M Hacker, James E Tomlinson, Gary A Wayman, Razia Sultana, Guy Chan, Enrique Villacres, Christine Disteché, and Daniel R Storm. Cloning, chromosomal mapping, and regulatory properties of the human type 9 adenylyl cyclase (adcy9). *Genomics*, 50(1):97–104, 1998.
- [99] Andrés Couve, Philip Thomas, Andrew R Calver, Warren D Hirst, Menelas N Pangalos, Frank S Walsh, Trevor G Smart, and Stephen J Moss. Cyclic amp–dependent protein kinase phosphorylation facilitates gabab receptor–effector coupling. *Nature neuroscience*, 5(5):415–424, 2002.
- [100] Jennifer Danielsson, Sarah Zaidi, Benjamin Kim, Hiromi Funayama, Peter D Yim, Dingbang Xu, Tilla S Worgall, George Gallos, and Charles W Emala. Airway epithelial cell release of gaba is regulated by protein kinase a. *Lung*, 194:401–408, 2016.
- [101] M Katherine Kelm, Hugh E Criswell, and George R Breese. The role of protein kinase a in the ethanol-induced increase in spontaneous gaba release onto cerebellar purkinje neurons. *Journal of neurophysiology*, 100(6):3417–3428, 2008.
- [102] Bernard J McDonald, Alessandra Amato, Christopher N Connolly, Dietmar Benke, Stephen J Moss, and Trevor G Smart. Adjacent phosphorylation sites on gabaa receptor β subunits determine regulation by camp-dependent protein kinase. *Nature neuroscience*, 1(1):23–28, 1998.
- [103] Kushal Kumar, Sorabh Sharma, Puneet Kumar, and Rahul Deshmukh. Therapeutic potential of gabab receptor ligands in drug addiction, anxiety, depression and other cns disorders. *Pharmacology Biochemistry and Behavior*, 110:174–184, 2013.
- [104] Sheila MS Sears and Sandra J Hewett. Influence of glutamate and gaba transport on brain excitatory/inhibitory balance. *Experimental Biology and Medicine*, 246(9):1069–1083, 2021.
- [105] Zachary D Brodник, Aashita Batra, Erik B Oleson, and Rodrigo A Espana. Local gabaa receptor-mediated suppression of dopamine release within the nucleus accumbens. *ACS chemical neuroscience*, 10(4):1978–1985, 2018.
- [106] Bradley M Roberts, Natalie M Doig, Katherine R Brimblecombe, Emanuel F Lopes, Ruth E Sid-dorn, Sarah Threlfell, Natalie Connor-Robson, Nora Bengoa-Vergniory, Nicholas Pasternack, Richard Wade-Martins, et al. Gaba uptake transporters support dopamine release in dorsal striatum with maladaptive downregulation in a parkinsonism model. *Nature communications*, 11(1):4958, 2020.
- [107] Mingzheng Wu, Zehua Li, Lei Liang, Pingchuan Ma, Dong Cui, Peng Chen, Genhao Wu, and Xue-Jun Song. Wnt signaling contributes to withdrawal symptoms from opioid receptor activation induced by morphine exposure or chronic inflammation. *Pain*, 161(3):532, 2020.
- [108] Xin Liu, Chilman Bae, Bolong Liu, Yong-Mei Zhang, Xiangfu Zhou, Donghang Zhang, Cheng Zhou, Adriana DiBua, Livia Schutz, Martin Kaczocha, et al. Development of opioid-induced hyperalgesia depends on reactive astrocytes controlled by wnt5a signaling. *Molecular Psychiatry*, 28(2):767–779, 2023.
- [109] Jeroen M Bugter, Nicola Fenderico, and Madelon M Maurice. Mutations and mechanisms of wnt pathway tumour suppressors in cancer. *Nature Reviews Cancer*, 21(1):5–21, 2021.

- [110] Jiaqi Liu, Qing Xiao, Jiani Xiao, Chenxi Niu, Yuanyuan Li, Xiaojun Zhang, Zhengwei Zhou, Guang Shu, and Gang Yin. Wnt/ β -catenin signalling: function, biological mechanisms, and therapeutic opportunities. *Signal transduction and targeted therapy*, 7(1):3, 2022.
- [111] Akira Nishi, Shusuke Numata, Atsushi Tajima, Xiaolei Zhu, Koki Ito, Atsushi Saito, Yusuke Kato, Makoto Kinoshita, Shinji Shimodera, Shinji Ono, et al. De novo non-synonymous tkl1xr1 mutation alters wnt signaling activity. *Scientific reports*, 7(1):2887, 2017.
- [112] Noboru Hiroi, Jennifer R Brown, Colin N Haile, Hong Ye, Michael E Greenberg, and Eric J Nestler. Fos b mutant mice: loss of chronic cocaine induction of fos-related proteins and heightened sensitivity to cocaine's psychomotor and rewarding effects. *Proceedings of the National Academy of Sciences*, 94(19):10397–10402, 1997.
- [113] Jianhua Zhang, Lu Zhang, Hongyuan Jiao, Qi Zhang, Dongsheng Zhang, Danwen Lou, Jonathan L Katz, and Ming Xu. c-fos facilitates the acquisition and extinction of cocaine-induced persistent changes. *Journal of Neuroscience*, 26(51):13287–13296, 2006.
- [114] Colleen A McClung and Eric J Nestler. Regulation of gene expression and cocaine reward by creb and δ fosb. *Nature neuroscience*, 6(11):1208–1215, 2003.
- [115] BA Nic Dhonnchadha, BF Lovascio, N Shrestha, A Lin, KA Leite-Morris, HY Man, GB Kaplan, and KM Kantak. Changes in expression of c-fos protein following cocaine-cue extinction learning. *Behavioural brain research*, 234(1):100–106, 2012.
- [116] Ming Xu. c-fos is an intracellular regulator of cocaine-induced long-term changes. *Annals of the New York Academy of Sciences*, 1139(1):1–9, 2008.
- [117] Huynh Nhu Mai, Yoon Hee Chung, Eun-Joo Shin, Naveen Sharma, Ji Hoon Jeong, Choon-Gon Jang, Kuniaki Saito, Toshitaka Nabeshima, Dora Reglodi, and Hyoung-Chun Kim. Il-6 knockout mice are protected from cocaine-induced kindling behaviors; possible involvement of jak2/stat3 and pacap signalings. *Food and Chemical Toxicology*, 116:249–263, 2018.
- [118] Fernanda Pedrotti Moreira, João Ricardo Carvalho Medeiros, Alfredo Cardoso Lhullier, Luciano Dias de Mattos Souza, Karen Jansen, Luis Valmor Portela, Diogo R Lara, Ricardo Azevedo da Silva, Carolina David Wiener, and Jean Pierre Oses. Cocaine abuse and effects in the serum levels of cytokines il-6 and il-10. *Drug and alcohol dependence*, 158:181–185, 2016.
- [119] Bruna S da Silva, Renata B Cupertino, Jaqueline B Schuch, Djenifer B Kappel, Breno Sanvicente-Vieira, Cibele E Bandeira, Lisia von Diemen, Felix HP Kessler, Eugenio H Grevet, Rodrigo Grassi-Oliveira, et al. The association between syt1-rs2251214 and cocaine use disorder further supports its role in psychiatry. *Progress in Neuro-Psychopharmacology and Biological Psychiatry*, 94:109642, 2019.
- [120] Thiago Wendt Viola, Jaqueline Bohrer Schuch, Diego Luiz Rovaris, Rafael Genovese, Lucca Tondo, Breno Sanvicente-Vieira, Aline Zaparte, Renata Basso Cupertino, Bruna Santos da Silva, Claiton Henrique Dotto Bau, et al. Association between cognitive performance and syt1-rs2251214 among women with cocaine use disorder. *Journal of Neural Transmission*, 126:1707–1711, 2019.
- [121] Anita Sidhu, Christophe Wersinger, CHARBEL E-H MOUSSA, and Philippe Vernier. The role of α -synuclein in both neuroprotection and neurodegeneration. *Annals of the New York Academy of Sciences*, 1035(1):250–270, 2004.
- [122] Yujing Qin, Qinjie Ouyang, John Pablo, and Deborah C Mash. Cocaine abuse elevates alpha-synuclein and dopamine transporter levels in the human striatum. *Neuroreport*, 16(13):1489–1493, 2005.
- [123] Tatiana Foroud, Leah Flury Wetherill, Tiebing Liang, Danielle M Dick, Victor Hesselbrock, John Kramer, John Nurnberger, Marc Schuckit, Lucinda Carr, Bernice Porjesz, et al. Association of al-

- cohol craving with α -synuclein (snca). *Alcoholism: Clinical and Experimental Research*, 31(4):537–545, 2007.
- [124] Chia-Hsiang Chen, Chia-Chun Huang, and Ding-Lieh Liao. Association analysis of gabrb3 promoter variants with heroin dependence. *PLoS One*, 9(7):e102227, 2014.
- [125] Ernest P Noble, Xuxian Zhang, Terry Ritchie, Bruce R Lawford, Stella C Grosser, Ross McD Young, and Robert S Sparkes. D2 dopamine receptor and gabaa receptor β 3 subunit genes and alcoholism. *Psychiatry Research*, 81(2):133–147, 1998.
- [126] Jiuzhou Song, Daniel L Koller, Tatiana Foroud, Kristie Carr, Jinghua Zhao, John Rice, John I Nurnberger Jr, Henri Begleiter, Bernice Porjesz, Tom L Smith, et al. Association of gabaa receptors and alcohol dependence and the effects of genetic imprinting. *American Journal of Medical Genetics Part B: Neuropsychiatric Genetics*, 117(1):39–45, 2003.
- [127] Ross McD Young, Bruce R Lawford, Gerald FX Feeney, Terry Ritchie, and Ernest P Noble. Alcohol-related expectancies are associated with the d2 dopamine receptor and gabaa receptor β 3 subunit genes. *Psychiatry research*, 127(3):171–183, 2004.
- [128] Arshad H Khan, Jared R Bagley, Nathan LaPierre, Carlos Gonzalez-Figueroa, Tadeo C Spencer, Mudra Choudhury, Xinshu Xiao, Eleazar Eskin, James D Jentsch, and Desmond J Smith. Genetic pathways regulating the longitudinal acquisition of cocaine self-administration in a panel of inbred and recombinant inbred mice. *Cell reports*, 42(8), 2023.
- [129] Bao-Zhu Yang, Shizhong Han, Henry R Kranzler, Lindsay A Farrer, and Joel Gelernter. A genomewide linkage scan of cocaine dependence and major depressive episode in two populations. *Neuropsychopharmacology*, 36(12):2422–2430, 2011.
- [130] Annalisa Buniello, Jacqueline A L MacArthur, Maria Cerezo, Laura W Harris, James Hayhurst, Cinzia Malangone, Aoife McMahon, Joannella Morales, Edward Mountjoy, Elliot Sollis, et al. The nhgri-ebi gwas catalog of published genome-wide association studies, targeted arrays and summary statistics 2019. *Nucleic acids research*, 47(D1):D1005–D1012, 2019.
- [131] Takuya Nishimura, Atsutaka Kubosaki, Yoichiro Ito, and Abner L Notkins. Disturbances in the secretion of neurotransmitters in ia-2/ia-2 β null mice: changes in behavior, learning and lifespan. *Neuroscience*, 159(2):427–437, 2009.
- [132] L David Porter, Hend Ibrahim, Lynn Taylor, and Norman P Curthoys. Complexity and species variation of the kidney-type glutaminase gene. *Physiological genomics*, 9(3):157–166, 2002.
- [133] Javier Márquez, José A Campos-Sandoval, Ana Peñalver, José M Matés, Juan A Segura, Eduardo Blanco, Francisco J Alonso, and Fernando Rodríguez de Fonseca. Glutamate and brain glutaminases in drug addiction. *Neurochemical research*, 42:846–857, 2017.
- [134] Manoranjan S D’Souza. Glutamatergic transmission in drug reward: implications for drug addiction. *Frontiers in neuroscience*, 9:404, 2015.
- [135] Michail Vikelis and Dimos D Mitsikostas. The role of glutamate and its receptors in migraine. *CNS & Neurological Disorders-Drug Targets (Formerly Current Drug Targets-CNS & Neurological Disorders)*, 6(4):251–257, 2007.
- [136] Camron D Bryant, Shoshana Eitan, Kevin Sinchak, Michael S Fanselow, and Christopher J Evans. Nmda receptor antagonism disrupts the development of morphine analgesic tolerance in male, but not female c57bl/6j mice. *American Journal of Physiology-Regulatory, Integrative and Comparative Physiology*, 291(2):R315–R326, 2006.

- [137] Hideaki Kato, Minoru Narita, Masami Suzuki, Kanji Yoshimoto, Masahiro Yasuhara, and Tsutomu Suzuki. Role of tyrosine kinase-dependent phosphorylation of nr2b subunit-containing nmda receptor in morphine reward. *Nihon Arukoru Yakubutsu Igakkai Zasshi= Japanese Journal of Alcohol Studies & Drug Dependence*, 42(1):13–20, 2007.
- [138] Michael C Salling, Alexander Grassetti, Vincent P Ferrera, Diana Martinez, and Richard W Foltin. Negative allosteric modulation of metabotropic glutamate receptor 5 attenuates alcohol self-administration in baboons. *Pharmacology Biochemistry and Behavior*, 208:173227, 2021.
- [139] Cassia N Cearley, Kelly Blindheim, Barbara A Sorg, James M Krueger, and Lynn Churchill. Acute cocaine increases interleukin-1 β mrna and immunoreactive cells in the cortex and nucleus accumbens. *Neurochemical research*, 36:686–692, 2011.
- [140] Jorge Montesinos, Estela Castilla-Ortega, Laura Sánchez-Marín, Sandra Montagud-Romero, Pedro Araos, María Pedraz, Óscar Porras-Perales, Nuria García-Marchena, Antonia Serrano, Juan Suárez, et al. Cocaine-induced changes in cx3cl1 and inflammatory signaling pathways in the hippocampus: Association with il1 β . *Neuropharmacology*, 162:107840, 2020.
- [141] Liang Liu, Mark R Hutchinson, Jason M White, Andrew A Somogyi, and Janet K Collier. Association of il-1b genetic polymorphisms with an increased risk of opioid and alcohol dependence. *Pharmacogenetics and genomics*, 19(11):869–876, 2009.